7-2-2018

Groundwater and Thermal Legacy of a Large Paleolake in Taylor Valley, East Antarctica as Evidenced by Airborne Electromagnetic and Sedimentological Techniques

Krista Falcon Myers
Louisiana State University and Agricultural and Mechanical College

GROUNDWATER AND THERMAL LEGACY OF A LARGE PALEOLAKE IN TAYLOR VALLEY, EAST ANTARCTICA AS EVIDENCED BY AIRBORNE ELECTROMAGNETIC AND SEDIMENTOLOGICAL TECHNIQUES

A Thesis

Submitted to the Graduate Faculty of the
Louisiana State University and
Agricultural and Mechanical College
in partial fulfillment of the
requirements for the degree of
Master of Science

In

The Department of Geology and Geophysics

by
Krista Falcon Myers
B.S., University of California, Santa Cruz, 2013
August 2018

ACKNOWLEDGMENTS

A special thanks to my graduate advisor, Peter Doran, for the unwavering support and guidance over the past 3 years, and my committee members Samuel Bentley and Suniti Karunatillake for the valuable discussion. Thank you to the co-authors of the SkyTEM project including Slawek Tulaczyk, Neil Foley, Hilary Dugan, Jill Mikucki, Ross Virginia, Esben Auken, Thue Bording, and Nikolaj Foged for helping with project development and data processing. Thank you to Jade Lawrence for her work in the field and invaluable edits and discussion at LSU. Thank you to all of the MCM LTER field team members for their contributions, specifically Maddie Myers, James McClure, Luke Winslow, Tony Bellagamba, Josh Darling, Heather Buelow, Maciek Obyrk, and Dimitri Acosta. Last but not least, I would like to thank my loving and supportive family for being the foundation of my success.

TABLE OF CONTENTS

ABSTRACT

During the Last Glacial Maximum, grounded ice in the Ross Sea extended into the otherwise ice-free McMurdo Dry Valleys, creating a series of large ice dammed paleolakes. Grounded ice within the mouth of Taylor Valley allowed for lake levels to reach elevations not possible at modern day and formed what is known as Glacial Lake Washburn (GLW). GLW extended from the eastern portion of Taylor Valley roughly 20 km west to a level ~300 m higher than modern day Lake Fryxell. The formation and existence of GLW has been debated, though previous studies correlate the timing of GLW with early Holocene grounded ice. Evidence of GLW has largely been constrained to the interpretation of glacial deposits and fluvial features such as lacustrine deposits, strandlines, and preserved paleodeltas. GIS and remote sensing techniques paired with regional resistivity data provide new insight into the paleohydrology of the region.

To quantify the extent of GLW, paleodelta locations were mapped using high resolution LiDAR digital elevation models and satellite imagery. Delta topset elevations were correlated between three streams in Fryxell basin to determine paleolake levels. Additionally, mean resistivity maps generated from airborne electromagnetic survey data (SkyTEM) reveal an extensive groundwater system within Fryxell basin which is interpreted as a legacy groundwater signal from GLW. Resistivity data suggests that active permafrost formation has been ongoing since onset of lake drainage, and that lake levels were over 60 m higher than modern only 1,000 – 2,000 yr BP. This coincides with a warmer than modern paleoclimate inferred by ice core records, indicating a dynamic hydrological system that is highly sensitive to small changes in climate. As global temperatures increase, Lake Fryxell will continue to experience highly variable lake levels. Lakes and groundwater within the McMurdo Dry Valleys are critical to understanding impacts on the broader ecosystem which is largely driven by the availability of liquid water.

INTRODUCTION

The McMurdo Dry Valleys (MDVs) are located within the Transantarctic Mountains and make up the largest ice-free region in Antarctica (Levy, 2013). Taylor Valley (TV), one of the southernmost valleys in the MDVs, extends west from the McMurdo Sound and terminates at the Taylor Glacier, an outlet glacier originating from the East Antarctic Ice Sheet. Due to its proximity to both the McMurdo Sound and a large outlet glacier, TV is a unique system influenced by both coastal climate and broader ice sheet dynamics (**Figure 1**).

Mean annual valley bottom temperatures range from -14.8 to -30°C (Doran et al., 2002) and the region receives between 3 – 50 mm water equivalent of precipitation per year (Fountain et al., 2010). Despite extremely low temperatures and minimal precipitation, the valleys are the site of a series of closed basin lakes fed by alpine glacier melt and snow via ephemeral streams (Chinn, 1987). Typical lakes in the MDVs contain 3 – 5 m perennial ice covers and vary in volume, chemistry, and biological activity (Lyons et al., 2000). During the austral summer, a short melt window occurs between December to February which accounts for most of the stream input

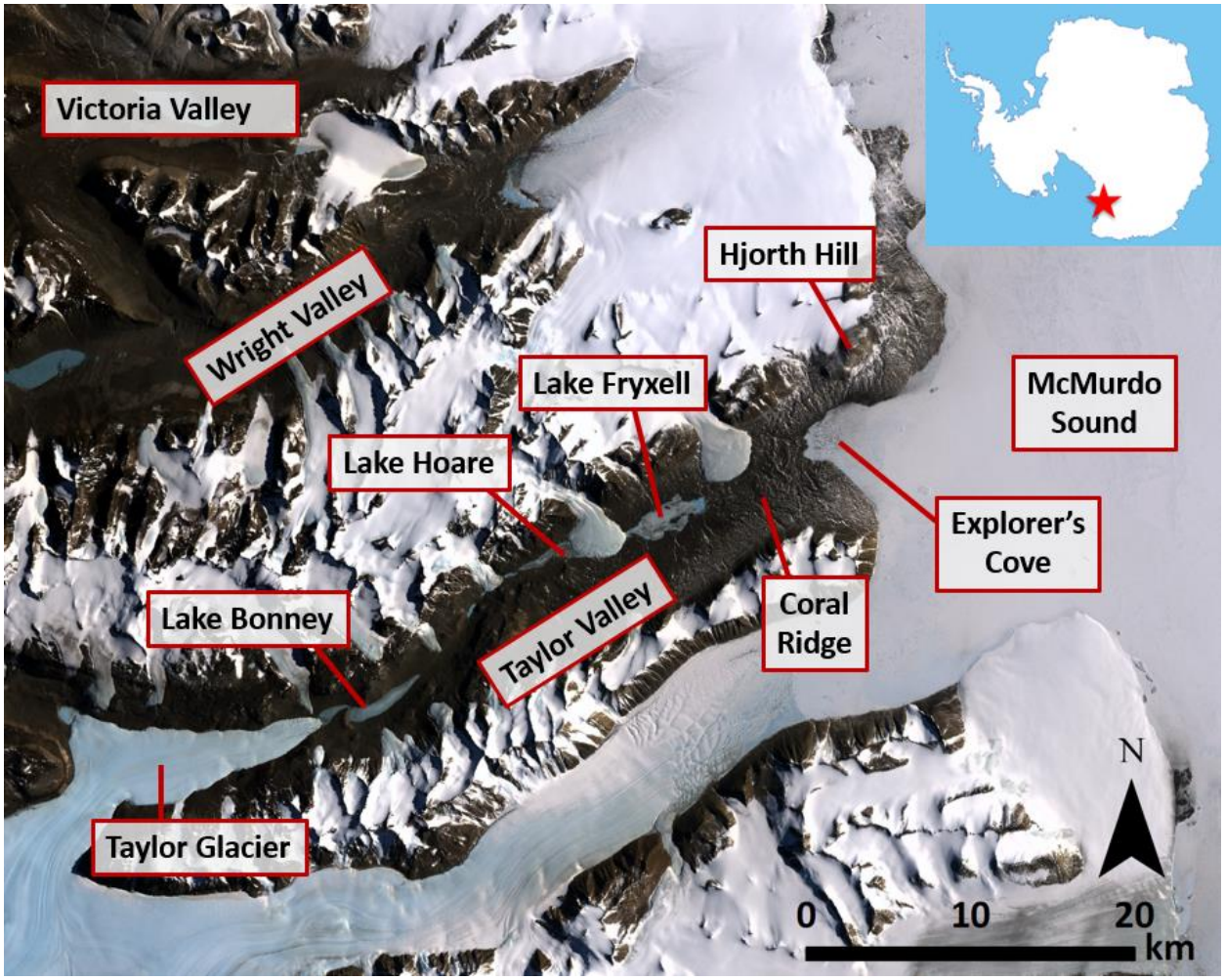

Figure 1. Overview map of the McMurdo Dry Valleys. Lake Fryxell is located in the eastern portion of Taylor Valley. Satellite imagery from Landsat Imagery Mosaic Antarctica (LIMA) published 2009.

(Chinn, 1987). Open water moats form around the perimeter of the lakes during the summer, and water loss occurs due to ablation of lake ice and evaporation of open water (Obryk et al., 2017).

The MDVs support a unique polar desert ecosystem that has been studied by the McMurdo Long Term Ecological Research (MCM LTER) project since 1992. Lake levels have been rising since the beginning of observational records starting in the early 1900s during the Scott expedition (Scott, 1905). Annual lake levels in TV have been recorded since the 1970s which provide a window into the dynamic climatic and geologic drivers of the MDV hydrologic system (Fountain et al., 2016). Lake Fryxell has risen by ~3 m since the 1970s and is characterized by high interannual variability in both lake level change (magnitude) and direction (rise versus fall) (Fountain et al., 2016). Fluctuating lake levels in the MDVs alters biological and chemical exchange between lakes, soils, and groundwater, making it critical for understanding MDV connectivity and ecosystem evolution. Additionally, isolated environments such as the MDVs offer a unique opportunity to study simplified physical and biological processes uninhibited by plant and animal influence, making them ideal proxies for planetary analogs (Doran et al., 1998; Dickinson and Rosen, 2003; Levy et al., 2009; Dickson et al., 2013).

AIMS AND OBJECTIVES

This study aims to quantify the extent and timing of lake levels within TV since the Last Glacial Maximum. Current understanding of lake level history in the MDVs is limited to surface observations (drifts, strandlines, paleodeltas, shallow soil chemistry) and paleohydrological models. Subsurface investigations are limited to the Dry Valleys Drilling Project in the 1970s, and due to increasingly strict environmental regulations, geophysical techniques can be utilized as a non-invasive method to peer below the surface. This study utilizes improved mapping of paleodeltas as indicators of lake level change paired with airborne electromagnetic survey data to study the thermal signature of a large paleolake recorded by permafrost and deep groundwater systems.

Not only does this study provide an independent method for constraining lake level history using permafrost age calculations, but also suggests recent mid to late Holocene lake level high stands which contradicts previous theories of a colder and drier era with little hydrologic activity throughout the last 5,000 years.

BACKGROUND

Ice Sheet History and Implications for Paleolake Evolution

Ice Sheet Advance During the LGM, Late Pleistocene (28,000 – 12,000 yr BP)

During the Last Glacial Maximum (LGM) roughly 28.5 – 12.8 kilo annum before present (ka BP) (Hall et al., 2015), Antarctica underwent a period of ice sheet thickening and advance. Stable isotope records from Taylor Dome (roughly 100 km west of TV) indicate lower mean annual air temperatures and a shift in atmospheric circulation patterns during the LGM (Steig et al., 2000) (**Figure 2**). This colder and drier period resulted in the advance of ice sheets and retreat of alpine glaciers in the MDVs (Steig et al., 2000). Ice from the East and West Antarctic ice sheets was grounded within the Ross Sea extending to the edge of the continental shelf, roughly 500 km further than the modern-day grounding line (Anderson et al., 2014).

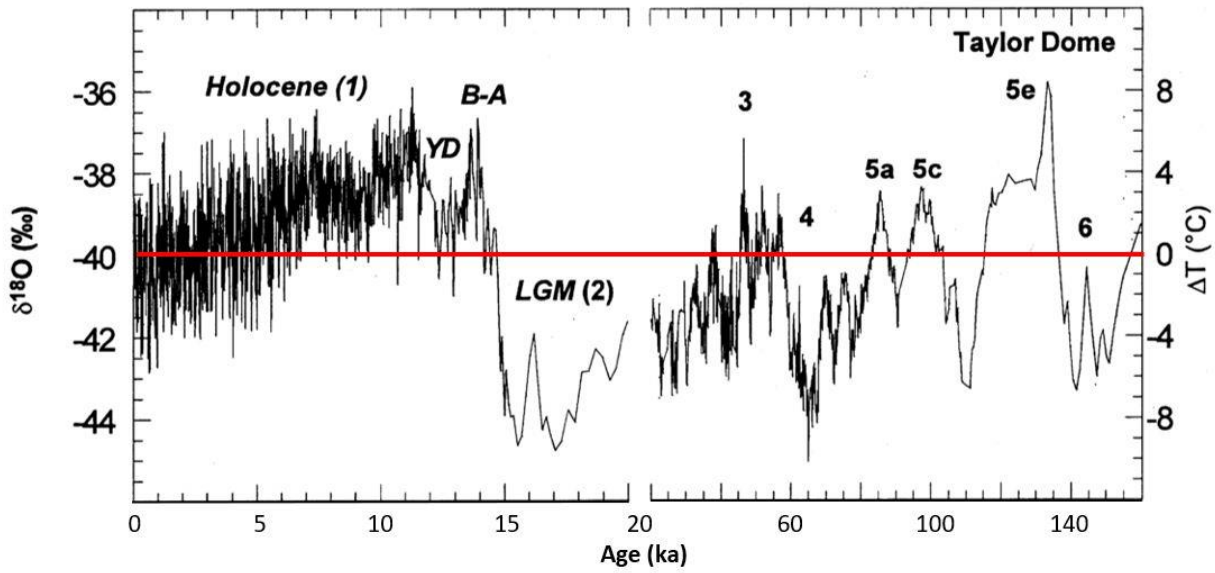

Figure 2. Stable isotope ($\delta^{18}O$) record from Taylor Dome ice core and paleotemperature reconstruction. A reference line for 0 ΔT (°C) is shown in red, representing deviation from modern temperatures. Modified from Steig et al. (2000).

During the LGM, ice originating from the Ross Ice Sheet (RIS) was grounded along the Ross Embayment (Denton and Marchant, 2000) and advanced into the McMurdo Sound approximately 26,860 ^{14}C yr BP (Denton and Marchant, 2000). The grounded ice flowed inland, spilling into the ice-free MDVs (**Figure 3**). The RIS remained grounded at a maximum equilibrium extent along the eastern side of the Transantarctic Mountains until roughly 12,700 ^{14}C yr BP (Hall and Denton, 2000).

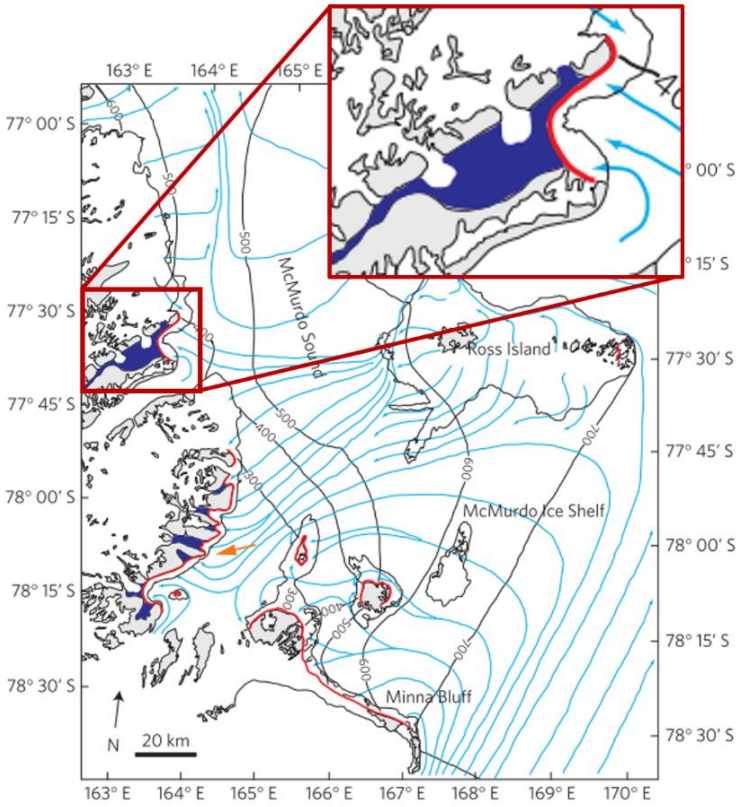

Figure 3. Grounded ice in Ross Sea forming ice dam (red line in inset), blocking drainage from Taylor Valley to the McMurdo sound forming GLW (inset). Paleolakes shown in dark blue. Modified from Hall et al.

Well-preserved geologic deposits provide evidence of grounded ice in the MDVs during the LGM (Hall and Denton, 2000; Denton and Marchant, 2000). The RIS transported glacial deposits referred to as the Ross Sea Drift which contain distinguishing kenyte erratics unique to Ross Island into the mouth of TV (Denton and Marchant, 2000). The RIS formed an ice face that reached to approximately 350 meters above sea level (masl) as evidence from a well-defined moraine ridge that merges with lacustrine deposits on the flank of Hjorth Hill at the mouth of TV (Denton and Marchant, 2000) (**Figure 1**). The moraine at Hjorth Hill represents the furthest extent of the grounded ice sheet into TV which existed between 14,602 - 12,785 ^{14}C yr BP (Hall and Denton, 2000).

The grounded ice in the mouth of TV allowed for lake levels to reach elevations that would otherwise not be possible without the RIS. Modern lake levels in TV are limited to a maximum elevation of ~78 to 81 masl (channel bottom and bank elevations, respectively) controlled by a topographic high near Coral Ridge, which acts as the divide between Fryxell basin and the McMurdo Sound (**Figure 1**). We bracket sill elevation to 78 – 81 masl since channel erosion rates and paleochannel depth are unknown. Bank elevation (81 masl) provides a conservative topographic threshold. By forming an ice wall that rose several hundred meters above the current topographic high at Coral Ridge, the grounded RIS allowed the formation of a large ice-dammed paleolake known as Glacial Lake Washburn (GLW) (**Figure 4**) (Denton and Marchant, 2000; Hall

and Denton, 2000). Large paleolakes also existed within Wright Valley (Hall et al., 2001), Victoria Valley (Hall et al., 2002), and Miers Valley (Clayton-Greene et al., 1988), providing further evidence of a widespread climatic and hydrological shift during the LGM.

MDV alpine glaciers are out of phase with the advance of large Antarctica ice sheets and retreated during the LGM (Stuiver et al., 1981; Denton et al., 1989; Hall and Denton, 2002). Alpine glaciers are fed through precipitation from open water evaporation in the McMurdo Sound. Because McMurdo Sound was iced over during the LGM, the alpine glaciers retreated (Dort, 1970; Stuiver et al., 1981; Denton and Marchant, 2000).

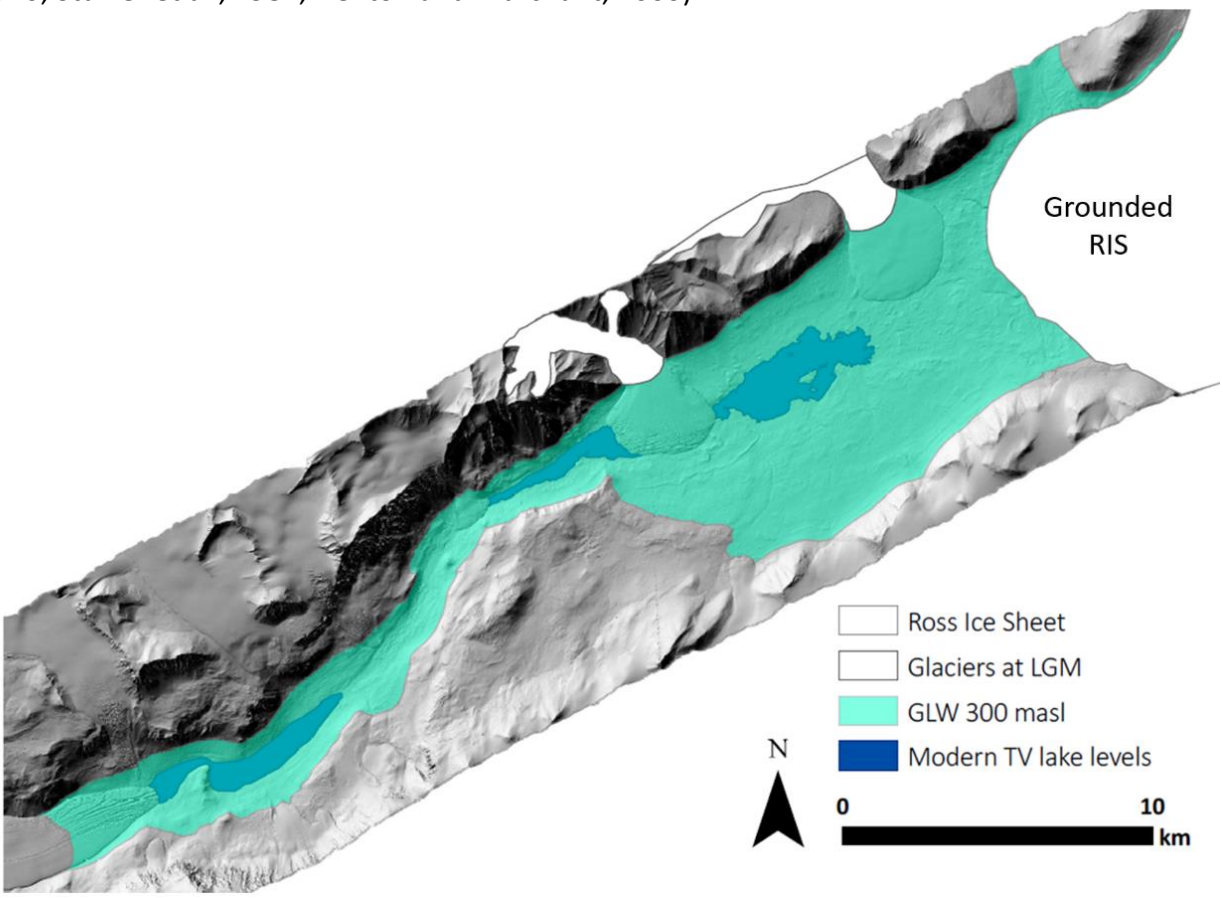

Figure 4. Glacial Lake Washburn extending up Taylor Valley (300 masl) during the LGM, between 28 to 12 ka BP. Modern day lake levels shown in dark blue. Extent of grounded Ross Ice Sheet is estimated from maps of Ross Sea Drift moraine locations (Hall and Denton, 2000). Extent of alpine glaciers (Canada and Commonwealth glaciers in white) are estimated. DEM (1 m resolution) is from 2014-15 LiDAR survey, accessed via OpenTopography (Fountain et al., 2017).

Deglaciation of the Ross Sea and Removal of RIS from Taylor Valley (12,000 – 8,000 yr BP)

During the late Pleistocene to early Holocene, grounded ice in the Ross Sea retreated from its maximum extent to near its modern day location (Anderson et al., 2014; Anderson et al., 2016). Radiocarbon dating of moraine deposits from the mouth of TV indicates that the surface

elevations of the grounded RIS did not lower until at least 10,800 ^{14}C yr BP (Hall and Denton, 2000; Denton and Marchant, 2000). The last evidence of grounded ice in TV was approximately 8,340 ^{14}C yr BP in the form of a delta deposit near Explorer's Cove (Stuiver et al 1981; Hall and Denton, 2000). The RIS remained grounded at Explorer's Cove between 8,340 – 5370 ^{14}C yr BP, and the region subsequently became a marine embayment (Hall and Denton, 2000).

Other studies suggest that the coastline of the MDVs was totally free of grounded ice around ~7.8 ka BP (Baroni and Hall, 2004) to ~8 ka BP (Hall et al., 2004). The grounding line retreated rapidly in the central and western portion of the McMurdo Sound beginning around 10 – 9 ka BP and continued until 8.3 – 8 ka BP (Anderson et al., 2016; Spector et al., 2017). Marine diatom records are in rough agreement with the timing of grounding line retreat around 12 - 6 ka BP (Cunningham et al., 1999).

During this transitional period of ice sheet thinning and retreat from the mouth of TV, deltas continued to form where streams entered the lake and deposited sediment. Paleodeltas represent periods of relatively stable lake levels, making them useful geomorphological markers of past lake levels. Timing and rate of lake level rise and drop remains largely unconstrained, however previous studies have utilized radiocarbon dating of algal mats (Hall and Denton, 2000) and optically stimulated luminescence (OSL) dating of quartz grains (Berger et al., 2013) to estimate the age of the paleodeltas. Hall and Denton (2000) found that almost all delta deposits within Fryxell basin are older than 8 ka BP (**Figure 5**) (Hall and Denton, 2000). Alternatively, Berger et al. (2013) determined that delta deposits are systematically younger than the ^{14}C dates at comparable elevations by ~5,000 yr. Further comparison of the two dating methods is discussed in subsequent sections.

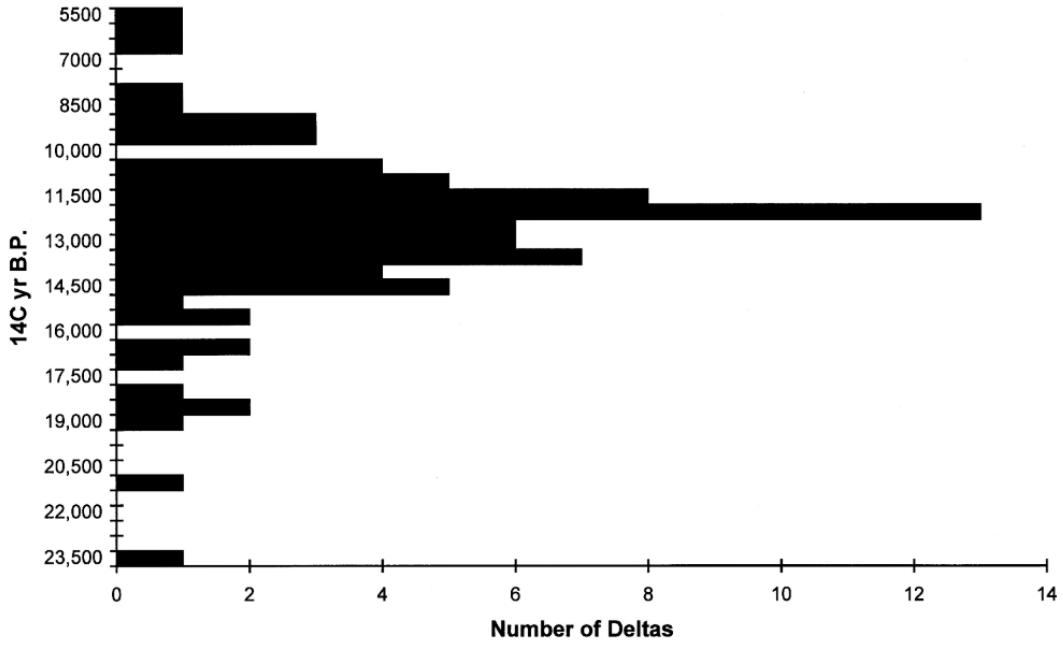

Figure 5. Frequency of midpoint radiocarbon dates from paleodeltas in Taylor Valley. Peak in number of deltas dated at 15,000 to 11,000 ^{14}C yr BP. Figure from Hall and Denton (2000).

Post-LGM Ice-free Conditions (8,000 yr BP to Present)

The rapid retreat of the RIS at the end of the LGM (~8 ka BP) led to the removal of the ice dam in the mouth of TV. Ice free conditions would have resulted in drainage of GLW, and subsequent lake levels would be limited by the 78 - 81 masl topographic constraint at Coral Ridge (**Figure 6**). Instead of contributing to lake level rise, any additional stream input would drain into the McMurdo Sound. During this time temperatures were at or above modern conditions. The paleoclimate record is marked by highly variable temperatures and a general cooling trend to modern conditions from 8 ka BP to present (Steig et al., 2000) (**Figure 2**). Alpine glaciers advanced to their current extent during the late Holocene, overriding Ross Sea Drift and GLW lacustrine deposits (Stuiver et al., 1981; Denton and Marchant, 2000; Higgins et al., 2000).

It was previously assumed that lake levels have remained near or below modern elevations over the last 5,000 yr because of a lack of sample yielding ages from this period for both ^{14}C and OSL (Hall and Denton, 2000; Berger et al., 2013). This study provides a third method for estimating lake level history during the previously unconstrained mid to late Holocene (5 ka to present).

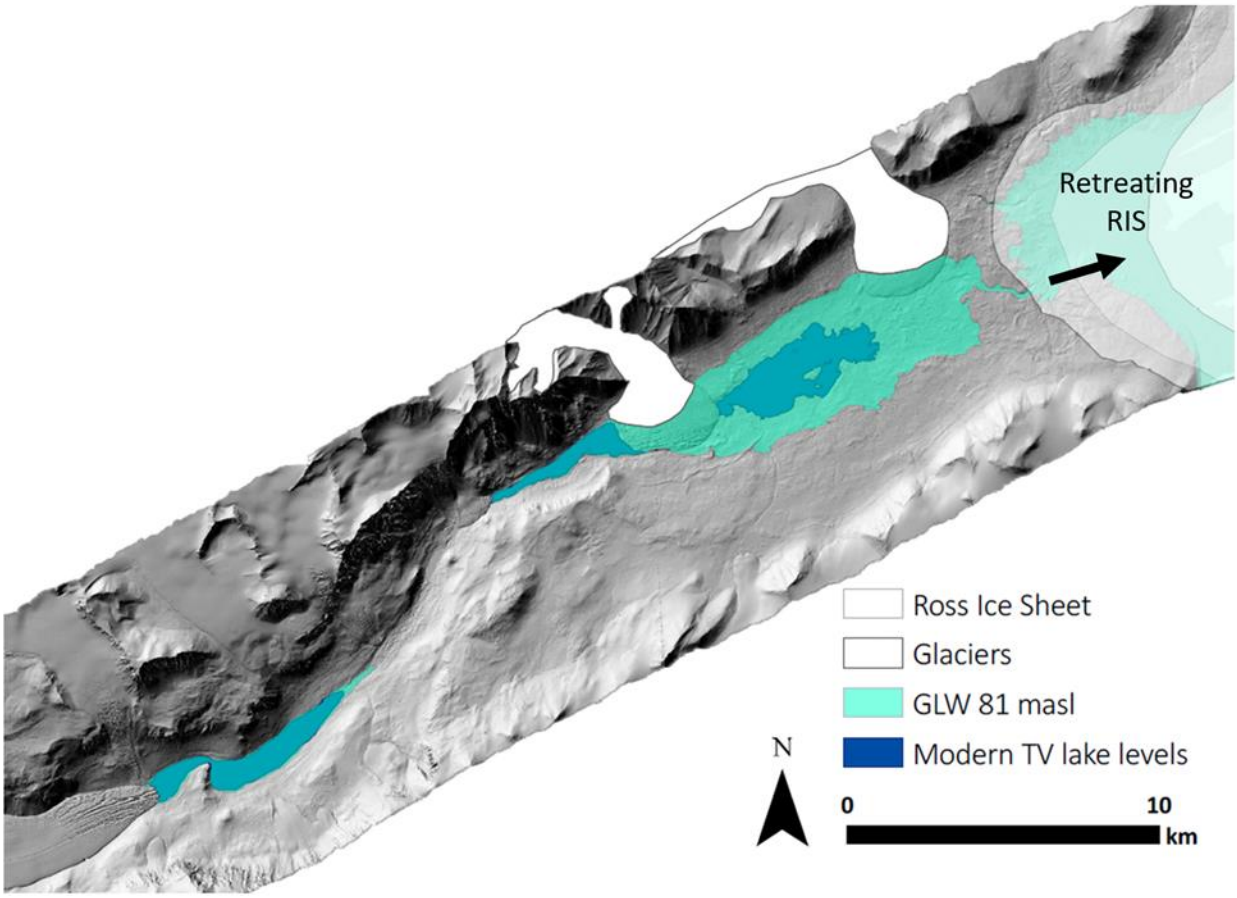

Figure 6. Glacial Lake Washburn at 81 masl during Late Pleistocene 12-8 ka BP. Modern day lake levels shown in dark blue. RIS retreated from mouth of TV ~8 ka BP. Extent of alpine glaciers (Canada and Commonwealth glaciers in white) are estimated. DEM (1 m resolution) is from 2014-15 LiDAR survey, accessed via OpenTopography (Fountain et al., 2017).

Lake Level History of Fryxell Basin

Lake Fryxell is one of the largest lakes in the Dry Valleys at roughly 5.5 km long and 22 m deep (**Figure 7**). Lake Fryxell is located between the Commonwealth and Canada Glaciers, two alpine glaciers that originate in the Asgard Range and extend into the center of TV. Lake Fryxell is a closed-basin lake sourced by glacial melt and snow delivered via 12 main streams. Ebnet et al. (2005) found that 89% of the 2001/2002 summer input into Lake Fryxell was from streams, and the remainder was from direct glacial melt from the Canada Glacier which abuts the western edge of the lake.

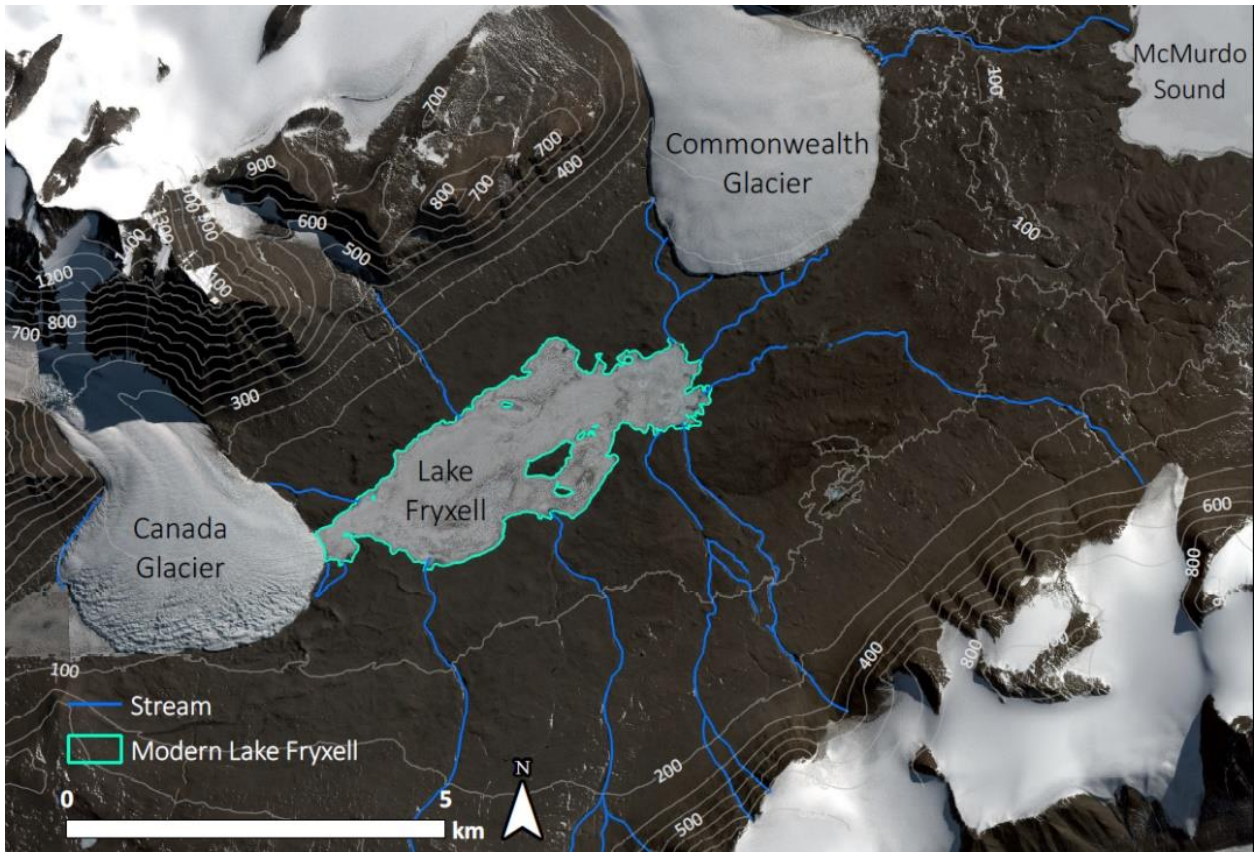

Figure 7. Modern Lake Fryxell located in the eastern Taylor Valley. 100 m elevation contours are shown in light grey. Satellite image taken by WorldView-3 satellite on Feb 2, 2017. Image © 2017 DigitalGlobe, Inc. provided by the Polar Geospatial Center.

Lake Fryxell has a 4 – 5 m thick perennial ice cover which varies year-to-year depending on surface ablation and ice formation on the underside of the ice cover (Dugan et al., 2013). Open water "moats" form around the perimeter of MDV lakes during summer months when temperatures are higher, and influx of stream flow further increases melt of lake ice (Hendy et al., 2000). Lake level measurements from 1972 to 2018 show that Lake Fryxell has undergone ~2.74 m of total lake level rise since measurements began, at an average rate of 5.57 cm/yr (**Figure 8**).

Summer temperature is the strongest driver of surface melt in the MDVs, and during the 2001/2002 austral summer there was an anomalously high number of degree days above freezing which resulted in 45 cm of lake level rise (**Figure 8**) (Doran et al., 2008). Compared to the average lake level rise over the past 46 yr record, the summer melt during the flood year was 815% higher than average. After the flood year, lake levels have been rising at a rate of approximately 10.31 cm/yr, roughly double the rate of the entire record. In the past three years (2015-2018) however, lake level rise has decreased to 2.18 cm/yr. The lake level record shows that high variability in lake levels over relatively short periods of time is typical for TV lakes.

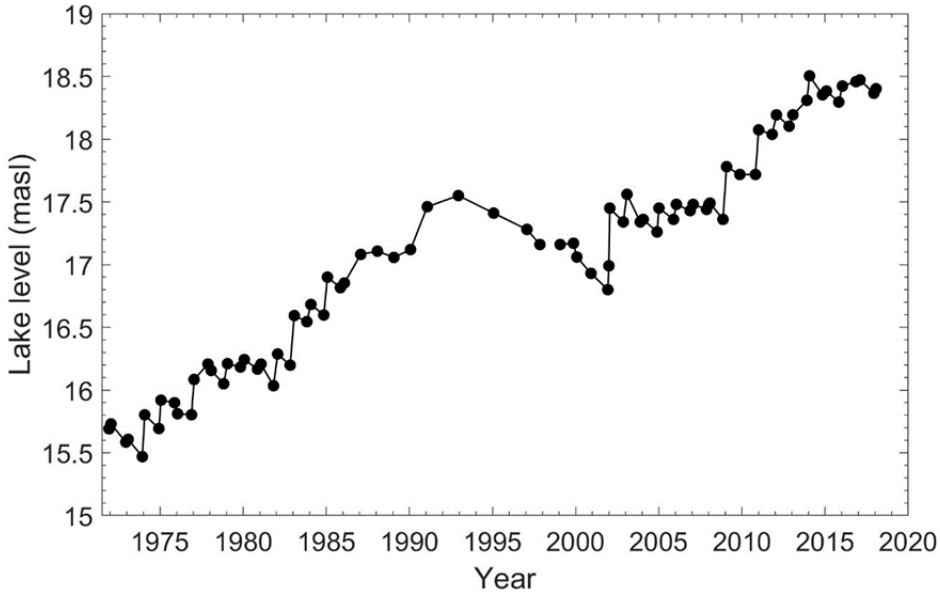

Figure 8. Elevation of Lake Fryxell from 1972 to 2018. Lake levels are determined by manual survey. Data provided by the MCM LTER (mcmlter.org).

These "flood years" might be the key to understanding how GLW could form during a glacial period generally categorized as colder and drier. The existence of a large paleolake during a period of colder temperatures and lower precipitation (Hall and Denton, 2000; Steig et al., 2000; Hall et al., 2002) is somewhat of a contradiction since this would require a sustained increase in meltwater input throughout its existence. Paleoclimate reconstruction from the Taylor Dome ice core record indicates that the region was between 4 to 8°C cooler than modern temperatures from 20 – 15 ka BP (**Figure 2**), however the period was marked by windier conditions (Steig et al., 2000). Obryk et al. (2017) calculates that increased frequency of warm down valley foehn winds could have account for enough melt generation to fill the western portion of TV (Lake Bonney basin). However, these calculations do not include the potential melt coming directly off the RIS (Obryk et al., 2017), which could account for the remaining amount of water necessary to fill TV to 300 masl assuming that the ice was grounded at Explorer's Cove (eastern TV) and not further inland as was suggested by Toner et al. (2013).

Some studies (Horsman, 2007; Arcone et al., 2008; Toner et al., 2013) suggest that GLW was much smaller, and only occupied western TV in Lake Bonney basin. Evidence of a smaller GLW includes lack of typical delta structure and stratigraphy as interpreted from ground penetrating radar surveys (Arcone et al., 2008, Horsman, 2007), and the lack of soluble salt

accumulation in soils in eastern TV (Toner et al., 2013). However, the correlation of paleoshorelines and delta deposits between streams suggest ubiquitously high lake levels throughout TV.

Deltas are actively forming at present day on all major streams that flow into Lake Fryxell and provide insight into how higher elevation paleodeltas may have formed. As the streams enter the lake, water velocity decreases resulting in sediment deposition and delta formation. Sediment transport and deposition rates remain unconstrained, however Hendy et al. (2000) suggests that polar lakes typically have high sediment loads despite their low flows. When lake level drops, the active stream channel incises the previously formed delta, leaving behind a perched deposit on the valley wall while a new delta forms at the subsequent lake level (**Figure 9**). Ancient delta deposits are common along streams in Fryxell basin and are interpreted as deposits that formed during relatively stable lake levels. Primary methods for dating paleodeltas in TV are radiocarbon dating of algal mats and OSL. Radiocarbon ages determined by Hall and Denton (2000) were corrected for atmospheric carbon levels using the CALIB 7.1 Radiocarbon Calibration program in order to compare to other methods (Stuiver et al., 2018). **Figure 10** shows atmospherically corrected ^{14}C ages compared to OSL ages. Both methods resulted in Pleistocene/Holocene ages, but the OSL dates are systematically younger than ^{14}C ages. The disagreement is likely due to the limitations of each method which are discussed below.

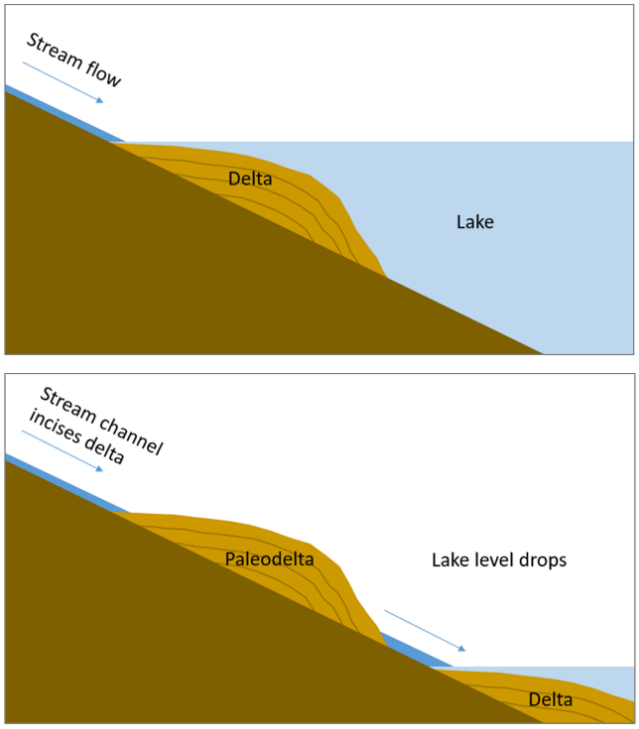

Figure 9. Schematic of paleodelta formation during higher lake levels. Sediment transported by streams is deposited during periods of relatively stable lake level forming a delta. As lake level drops, the stream channel incises the delta and a new delta forms at subsequent lake level.

Limitations of Lake Level Dating Methods – ^{14}C and OSL

Radiocarbon dating of Antarctic marine sediments is affected by a large ^{14}C reservoir effect due to extremely old Southern Ocean waters (Hall, 2009). Additional factors that influence the marine reservoir effect include low amounts of organic content in the region compounded with the reworking of old carbon in the system (Hall, 2009), and a modern marine reservoir effect is estimated to be ~1,130 +/- 200 yrs (Reimer et al., 2004).

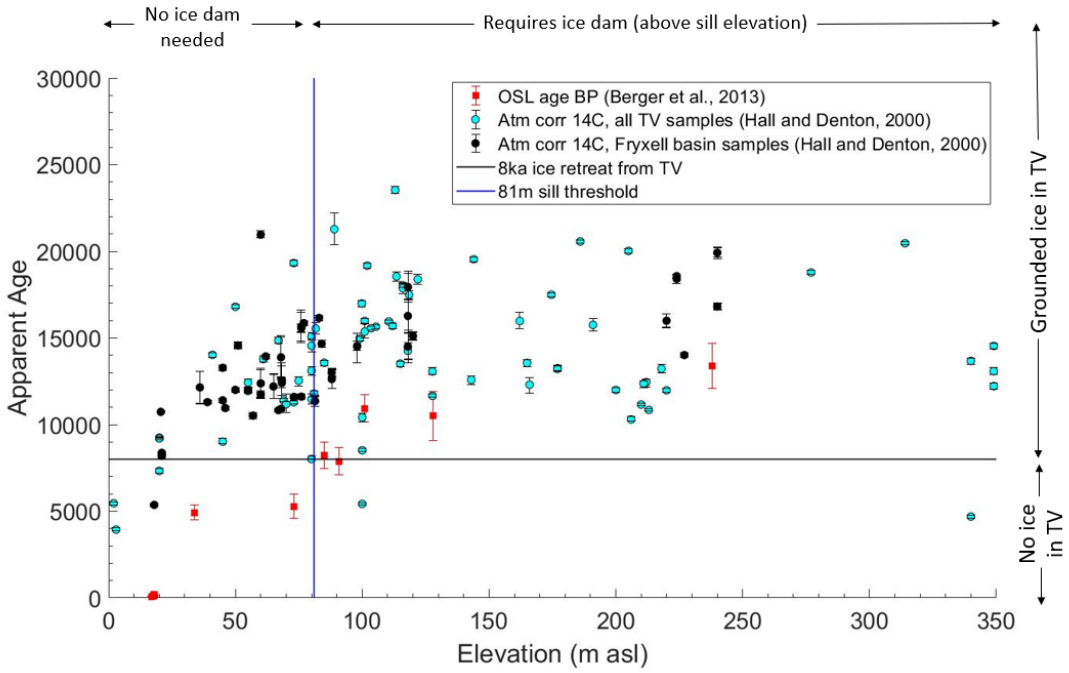

Figure 10. Age of delta deposits from ^{14}C dating of preserved algal mats (Hall and Denton, 2000) shown as circles. Samples from all of Taylor Valley and just Fryxell basin shown as black and cyan circles, respectively. Age estimates using optically stimulated luminescence (OSL) dating shown as red squares (Berger et al., 2013). Black line represents retreat of grounded Ross Ice Sheet from the mouth of Taylor Valley (~8 ka BP), blue line represents approximate elevation of sill at Coral Ridge (81 masl).

Terrestrial deposits are also influenced by reservoir carbon effects (i.e. older dissolved organic carbon (DIC) sources), however deposits along streams flowing into shallow moats are considered to have been well-mixed and equilibrated with atmospheric carbon (Doran et al., 1999; Hall and Denton, 2000; Hendy and Hall, 2006; Hall, 2009; Doran et al., 2014). Previous studies dating lacustrine deposits from the MDVs do not correct or a reservoir effect (Hall and Denton, 2000). However, if the RIS was a significant source of GLW water (Obryk et al., 2017), algal mats forming in waters directly sourced by the RIS may have experienced a reservoir effect from the old DIC incorporated at the time of RIS ice formation (Hall and Henderson, 2001). This would require a large reservoir correction which has yet to be quantified or addressed in previous literature. Another possible source of error is that it is unknown whether or not algal mats found in the paleodelta deposits were formed in situ or transported from within the stream channel

and later buried by sediment. Algal mats may not be a reliable indicator of lake age, but ^{14}C dates can be used as an upper bound for GLW timing during and after the LGM.

The second method considered in this study is OSL dating conducted by Berger et al. (2013). OSL determines the last time a quartz grain was exposed to solar irradiation, providing estimated burial age. Although unaffected by carbon sources, OSL has limitations as well that must be considered. OSL determines burial timing which does not necessarily reflect the deposition age of the sediment and is a function of paleodelta sediment accumulation rate which is unknown. Therefore, OSL may underestimate the age of delta formation. OSL dates are on average ~5,205 yrs younger than ^{14}C samples from Fryxell basin (**Figure 10**).

Samples collected at modern lake elevations (~18 masl) were determined to be 55 +/- 55 yr BP by OSL methods, but Hall and Denton (2000) date a delta at the same elevation to be 5,367 +/- 78 yr BP. The 5,312 +/- 133 yr discrepancy between samples that appear to have been collected from modern lake elevation may provide a rough estimate of the radiocarbon reservoir effect for paleodeltas in TV.

Groundwater and Permafrost in Lake Fryxell Basin

A recent airborne resistivity survey, SkyTEM, revealed an extensive groundwater system extending throughout TV, possibly connecting to the McMurdo Sound (Mikucki et al., 2015) (**Figure 11**). Prior to the SkyTEM surveys, groundwater studies were limited to the Dry Valleys Drilling Project (DVDP) conducted in the 1970s and studies on shallow groundwater systems within the active layer, which is defined as the seasonally-thawed upper layer of soil in regions of permafrost (Levy et al., 2011; Gooseff et al., 2013).

Active layer depths range from 25 to 45 cm within TV (Bockheim et al., 2007). Calculated active layer water fluxes are two orders of magnitude smaller than glacial stream discharge (Cartwright and Harris, 1981), and are therefore considered relatively unimportant in the water budget of MDV lakes (Doran et al., 1999). Previous studies rely on the geochemistry of MDV lakes to constrain groundwater fluxes; however, most studies conclude that groundwater contribution to lakes is minimal. However the MDV ecosystem is largely driven by liquid water availability which makes these groundwater systems a potentially significant habitat for microbial communities.

Permafrost is ubiquitous throughout the MDVs and is defined as substrate that is at or below 0°C for more than two years, regardless of degree of saturation (McGinnis and Jensen, 1971). Permafrost can further be broken into subgroups, depending on degree of saturation and confining properties. Confining permafrost does not allow any fluid flow, whereas aquifrost is permafrost that allows groundwater flow due to local conditions such as salinity and porosity (McGinnis and Jensen, 1971). Confining layer permafrost tends to have much higher electrical resistivities (<10,000 Ωm) than aquifrosts (50 - 1,000 Ωm) depending on temperature and degree of saturation of the aquifrost (McGinnis and Jensen, 1971).

Shallow confining permafrost can facilitate active layer flow above the ice boundary (Gooseff et al., 2013). Mapping of shallow active layers within the MDVs indicates that 67% of TV is occupied by dry frozen permafrost (<5% water content) and the remaining 33% is occupied by ice-cemented permafrost (≥5% water content) (Bockheim et al., 2007). The eastern portion of TV

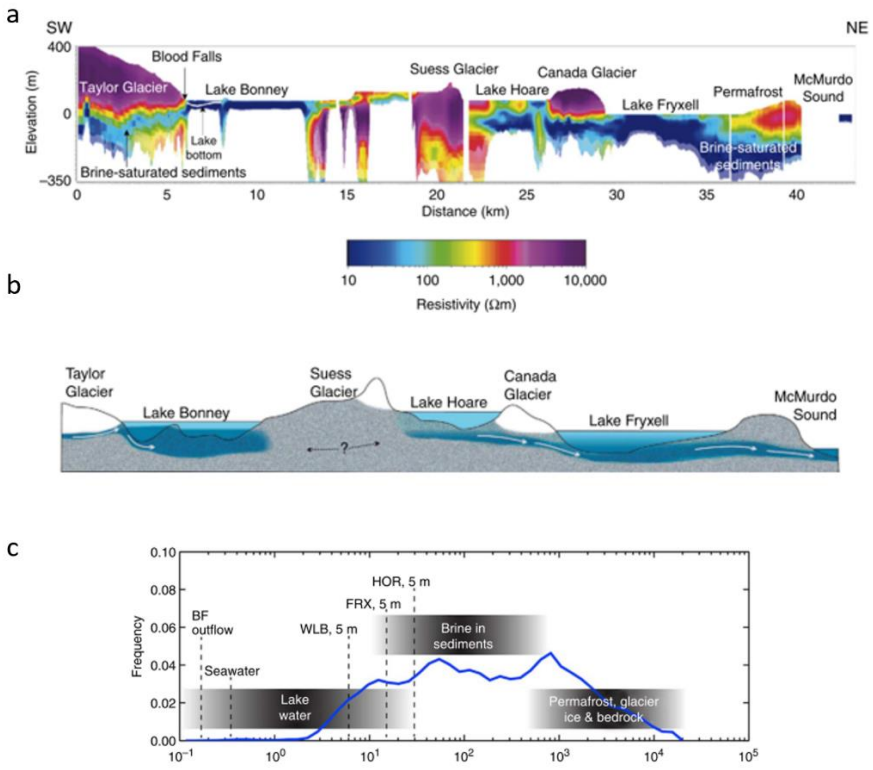

Figure 11. (a) Airborne electromagnetic (AEM) sensor, SkyTEM, show regions of low resistivity extending throughout Taylor Valley. (b) Conceptual model of connection between lakes and deep saline groundwater systems. (c) Resistivity interpretations; <10 Ωm is interpreted as lake water, 10 to 1,000 Ωm as brine in sediments, and >1,000 Ωm as permafrost, glacier ice or bedrock. Figure modified from Mikucki et al. (2015).

including Fryxell basin is primarily ice cemented permafrost, which is characteristic of younger soils (Bockheim et al., 2007). Deep permafrost in the MDVs was previously considered relatively stable with the exception of thermokarst on stream channels and other steep topographic features (Sudman et al., 2017). Thermokarst occurs when permafrost degrades and destabilizes causing slumping and erosion. Channel erosion rates caused by thermokarst can be as high as 20 cm/yr in TV streams (Sudman et al., 2017). Although surficial, this phenomenon is an important contributor to stream sediment fluxes and channel destabilization.

The DVDP used sedimentological and geophysical techniques to determine characteristics of deep groundwater and permafrost in the MDVs. McGinnis and Jensen (1971) recognized the presence of groundwater signals emanating from lakes known as taliks (unfrozen zones within permafrost due to the presence of a lake). However, these studies were limited to only a handful of measurements in TV and did not address the thermal effect of past higher lake levels on the modern permafrost signature. This study is the first to map permafrost thickness and distribution in eastern TV, which can provide valuable insight into the paleohydrology and general connectivity of the MDV hydrologic system. The relationship between permafrost and deep groundwater systems has been largely unexplored but may be a critical component to understanding landscape evolution of the MDVs.

METHODS

Paleodelta Mapping

Two seasons of field work were conducted in 2015/16 and 2016/17 to map paleodeltas across three streams (Delta Stream, Crescent Stream, and Huey Creek) in Fryxell basin (**Figure 7**). Paleodelta locations have been previously mapped in other studies (Hall and Denton, 2000), however this is the first study to use high resolution remote sensing data paired with centimeter scale precision differential GPS (provided by UNAVCO) to fully map the distribution of paleodelta deposits within Fryxell basin. High resolution multispectral satellite imagery (WorldView3, DigitalGlobe, 2017) and high resolution LiDAR digital elevations models (DEMs) (Fountain et al., 2017) were imported into ArcMap and used to map elevations and extents of paleodeltas within Fryxell basin (**Figure 12**). Field mapping was used to ground truth mapping done in ArcGIS. Some paleodeltas were indistinguishable in the field and could only be identified using DEMs, or vice versa. Paleodeltas are characterized by gently sloping deposits along stream channels that are generally lighter toned fans that widen on the downstream side. Surfaces of deltas are armored by aeolian sorted gravels and typically lack large boulders in comparison to the surrounding landscape, and degree of preservation is highly variable. Well-preserved deltas have defined topsets and foresets and have typical deltaic fan morphology, whereas poorly-preserved deposits are characterized as elongated mounds on the stream banks with little to no fan morphology (**Figure 12**).

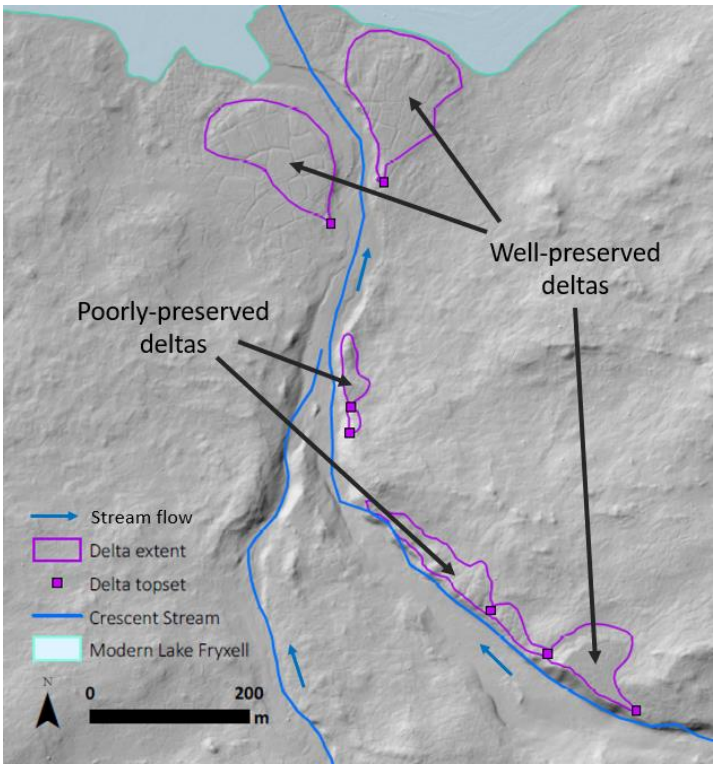

Figure 12. Mapping of paleodeltas along Crescent Stream on the southern valley wall of Lake Fryxell basin. Paleodelta extents outlined in purple, and topset locations shown as squares. DEM (1 m resolution) is from 2014-15 LiDAR survey, accessed via OpenTopography (Fountain et al., 2017).

In order to reconstruct past lake level high stands, the initiation point of each topset (where the stream would have entered the lake) was mapped in ArcGIS. An example of paleodelta topset mapping is shown in **Figure 12**. Delta topset elevations were correlated across three streams using a squared Euclidean distance metric to minimize variance within each grouping. The elevation of each paleolake level was then plotted as a contour of constant elevation. Lake levels were not corrected for isostatic rebound resulting from drainage of GLW and removal of the RIS from the mouth of TV. Previous work utilizes paleoshorelines to determine isostatic rebound rates (Konfal et al., 2013), and found that MDV shorelines are dipping SE, which is contrary to predicted western rebound directions that would have resulted from the unloading of ice in the Ross Sea. Since the rebound direction is perpendicular to the valley orientation, we do not correct for these, however isostatic rebound may still be a source of error for paleodelta elevations.

SkyTEM Resistivity Surveys

SkyTEM, a time-domain airborne electromagnetic (AEM) sensor system, was flown over TV in 2011. A transmitter generated a pulsed primary magnetic field which then induced eddy currents in the subsurface (**Figure 13**). The secondary magnetic field generated in the subsurface was measured by an induction receiver coil (Foley et al., 2016). The apparent conductivity can be determined using the primary field decay equation (Ward and Hohmann, 1988). The 2011 AEM survey collected 560 km of resistivity data in eastern TV. Flight lines were approximately 500 m apart, and nodes (individual sounding points) were collected every ~25 m along each flight line (**Figure 14**).

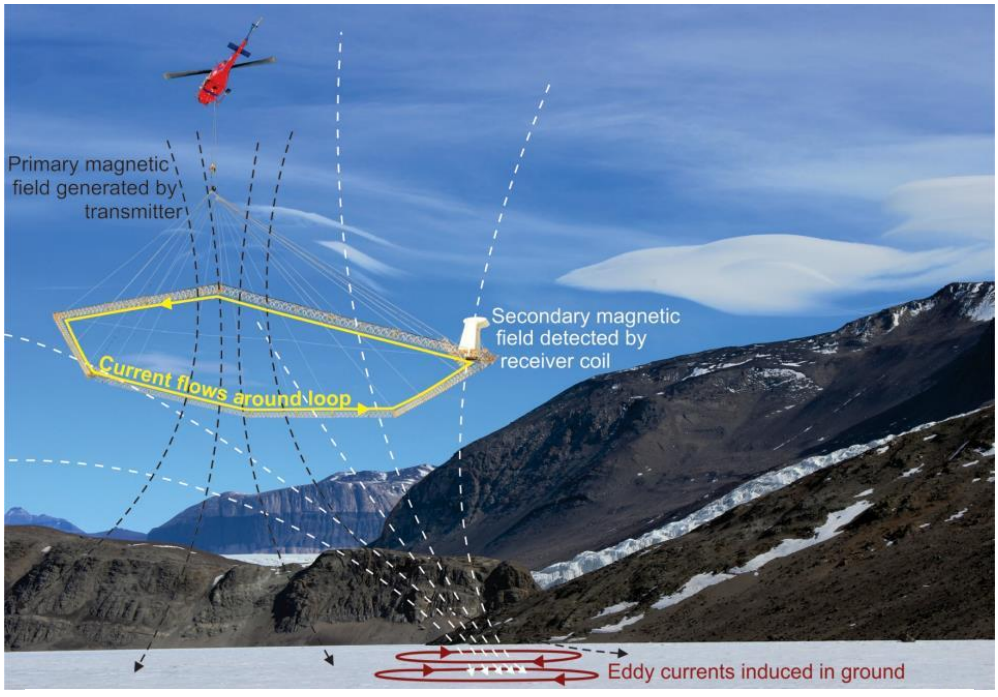

Figure 13. Rendition of SkyTEM airborne electromagnetic sensor over Lake Bonney. Figure from Mikucki et al. (2015) supplemental information.

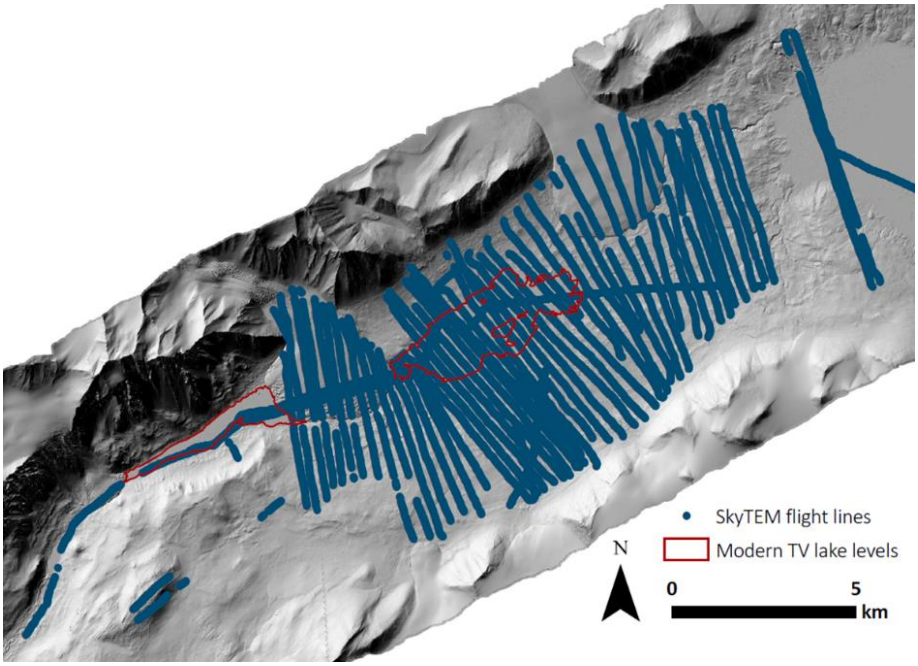

Figure 14. Map of SkyTEM resistivity survey coverage collected in 2011. Lake Fryxell and Lake Hoare outlined in red. DEM (1 m resolution) is from 2014-15 LiDAR survey, accessed via OpenTopography (Fountain et al., 2017).

Specialized inversion software, Workbench, was developed by the University of Aarhus to process raw resistivity data and create resistivity inversions (Foley et al., 2016). Mean resistivity maps were generated in Workbench using a spatially constrained inversion of the data from Fryxell basin. Five meter thick slices of constant elevation from 250 masl to -300 masl were interpolated to generate mean resistivity maps using a 1,000 m search radius and kriging interpolation. Mean resistivity maps were imported into ArcGIS to overlay on top of the DEMs and satellite imagery to map location and extent of low resistivity regions. The depth of investigation (DOI) is determined in Workbench and represents the depth of reliable resistivity data. Regions of low resistivity (<1,000 Ωm, typical of lake water and brine saturated sediments) have lower DOIs (<100 m) due to signal attenuation, whereas regions of high resistivity (>1,000 Ωm, typical of permafrost and bedrock) can penetrate much deeper (>300 m) (Mikucki et al., 2015; Foley et al., 2016).

Subsurface characteristics and chemistry can be inferred from the relationship of resistivity to temperature, salinity, porosity, and degree of saturation (Mikucki et al., 2015). The regions of low resistivity underlying higher resistivities are interpreted as liquid brine saturated sediments capped by permafrost and represent groundwater extent in Fryxell basin.

In order to calculate permafrost freeze-back rates of the recently exposed valley floor, a general layer search was conducted to extract depth to brine values. Depth to brine can also be thought of as the thickness of permafrost above the low resistivity groundwater system. These values are determined by assigning a resistivity threshold of 100 Ωm to delineate the boundary between permafrost and brine saturated sediment (Mikucki et al., 2015). This is in rough agreement with resistivity values of saturated sediment first explored in the 1970s as part of the

DVDP (McGinnis and Jensen, 1971). Saturated samples range from 78 to >500,000 Ωm at 21 and -25°C respectively (McGinnis and Jensen, 1971), indicating that 100 Ωm is a reasonable boundary to use for unfrozen sediments from TV that are close to 0°C.

Workbench was used to export location (X and Y values in m, UTM58S), elevation (Z in masl), and depth to brine (d in meters) for each node point of SkyTEM data. Depth to brine values for each node were interpolated to map distribution of the permafrost/brine boundary. Depth to brine maps were smoothed using a low pass filter in ArcGIS to reduce noise, which is particularly high around the edges where data density is lower.

Permafrost thickness, which is the same as the depth to 100 Ωm boundary, was used to calculate time since initiation of permafrost freeze-back resulting from lake drainage using Equation 1 adapted from Osterkamp and Burn (2003)

$$t = s\frac{d^2 \cdot H_s}{2k_b \cdot (-T_{ps})} \quad \text{[Eq 1]}$$

where t is the age of permafrost in seconds, s is a conversion factor from seconds to years, d is the thickness of permafrost (m), H_s is the volumetric latent heat of fusion for sediments corrected for porosity in Joules per cubic meter (J/m^3), k_b is the bulk thermal conductivity of permafrost in watts per meter per Kelvin (W/mK), and T_{ps} is the temperature difference between the atmosphere and permafrost freezing front (K). The volumetric latent heat of fusion for sediments corrected for porosity is estimated using Equation 2

$$H_s = H_v \cdot \varphi \cdot (1 - \varphi_a) \quad \text{[Eq 2]}$$

where H_v is the volumetric latent heat of the sediments (3.34e+6 J/m^3), φ is the porosity of the sediment, and φ_a is the percent air in pore space.

Bulk thermal conductivity of permafrost (k_b) is estimated using Equation 3

$$k_b = {k_m}^{1-\varphi} \cdot {k_f}^{\varphi(1-\varphi_a)} \cdot {k_a}^{\varphi \cdot \varphi_a} \quad \text{[Eq 3]}$$

where k_m is the thermal conductivity of the matrix, k_f is the thermal conductivity of the fluid, and k_a is the thermal conductivity of air. All thermal conductivity terms are in units of W/mK.

In order to calculate a range of possible permafrost ages for each elevation, a Monte Carlo statistical analysis was performed. Each input variable was assigned a percent variance (standard deviation), which was then multiplied by an independently varied random number and added to the original input and repeated for 10,000 iterations. φ, φ_a, T_{ps}, and k_m were assigned a standard deviation of 20%, and k_f and k_a were assigned a standard deviation of 2% since they are better constrained. We calculate permafrost age assuming completely saturated sediment ($\varphi_a = 0$) as well as partially saturated sediment ($20\% \leq \varphi_a \leq 24\%$). This approach assumes a normal distribution of all data, and a homogenous substrate in both space and time for simplification purposes.

To produce the upper bound of permafrost ages, Eq 1 was calculated using the maximum or minimum possible value for each input variable. H_s was maximized by assigning a maximum φ (adding one standard deviation), with and without air in the pore space. Minimum k_b was calculated by minimizing k_m by subtracting one standard deviation and maximizing φ by adding one standard deviation, with and without air in pore space. T_{ps} was minimized by adding one standard deviation from the average value. Values for each variable are summarized in **Table 1**.

Table 1. Input values for Equations 1 – 3.

Variable	Average value (fully saturated)	Max value (fully saturated)	Average value (partially saturated)	Max value (partially saturated)	Description
φ	0.30	0.36	0.30	0.36	Porosity
$φ_a$	0	0	20	24	% Air in pore space
H_s	1.002e+8	1.202e+8	8.016e+7	9.138e+7	vol. heat of fusion (J/m^3)
k_f	2.250	2.205	2.250	2.205	TC of fluid (W/mK)
k_m	3.5	2.8	3.5	2.8	TC of matrix (W/mK)
k_a	--	--	0.0236	0.0231	TC of air (-10°C) (W/mK)
k_b	3.066	2.569	2.332	1.733	Bulk TC (W/mK)
T_{ps}	-15	-12	-15	-12	Temp difference (K)

Lake taliks (unfrozen zones within regions of permafrost) allow connection between lakes and deep groundwater systems. The formation of taliks beneath a polar lake depends on lake radius, bottom water temperature, mean annual air temperature, and the geothermal gradient. A first order estimate to determine whether or not a talik can exist in modern conditions, we used Equation 4 to estimate the thermal profile beneath a lake;

$$T_z = T_{air} + \frac{z}{\left(\frac{dT_{geo}}{dz}\right)} + (T_{bot} + T_{air}) * \left(1 - \frac{z}{\sqrt{z^2+r^2}}\right) \quad \text{[Eq 4]}$$

where T_z is the temperature at depth z (°C), z is depth below surface (m), $\frac{dT_{geo}}{dz}$ is the geothermal gradient (50 m/°C), T_{bot} is the temperature of lake bottom water, and r is the radius of the lake. This equation can be simplified for a region without a lake using Equation 5;

$$T_z = T_{air} + \frac{z}{\left(\frac{dT_{geo}}{dz}\right)} \quad \text{[Eq 5]}$$

For modern Lake Fryxell, T_{air} is -18°C, T_{bot} is 2°C, and r is 1.7 km (north-south length of lake).

RESULTS

Paleodeltas were mapped across three streams in Fryxell basin to reconstruct paleolake elevations (**Figure 15**). Twenty seven delta topset elevations resulted in 8 paleolake levels which range from 125 to 24 masl. The number of paleodeltas within each group was as few as one delta (98 masl) to five deltas (24 and 87 masl). 74% of the paleodeltas within Lake Fryxell basin are below the 81 masl sill level. The 24 masl level (red contour in **Figure 15**) has one of the strongest clustering of delta elevations across all three streams. The 44 masl level (orange contour in **Figure 15**) also has strong correlation across all three streams. From 59 to 125 masl there is a large spread in paleodelta elevations across the three streams (**Figure 16**).

Most of the deltas were armored by aeolian sorted gravels and some had internal carbonate cementation; however, delta preservation and area are probably a function of lake level duration, sediment accumulation rate, erosion rates and number of times a lake has reached that elevation throughout multiple cycles of rise and fall. Delta Stream was the only stream that had paleodeltas above 100 masl.

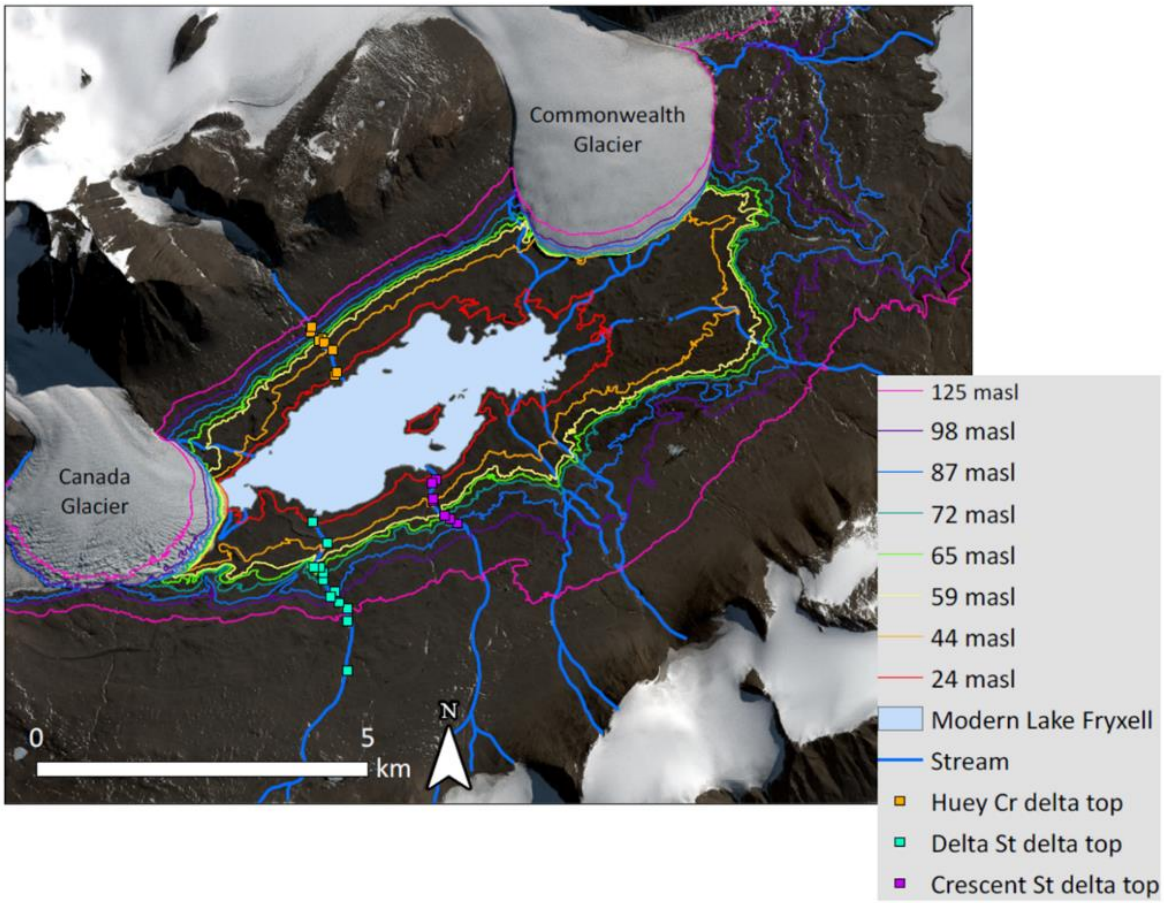

Figure 15. Estimated paleolake highstands determined from mapping of paleodelta topsets. Paleolake elevations plotted as contours of constant elevation. Satellite image taken by WorldView-3 satellite on Feb 2, 2017. Image © 2017 DigitalGlobe, Inc. and data provide Polar Geospatial Center. DEM (1 m resolution) is from 2014-15 LiDAR survey, accessed via OpenTopography (Fountain et al., 2017).

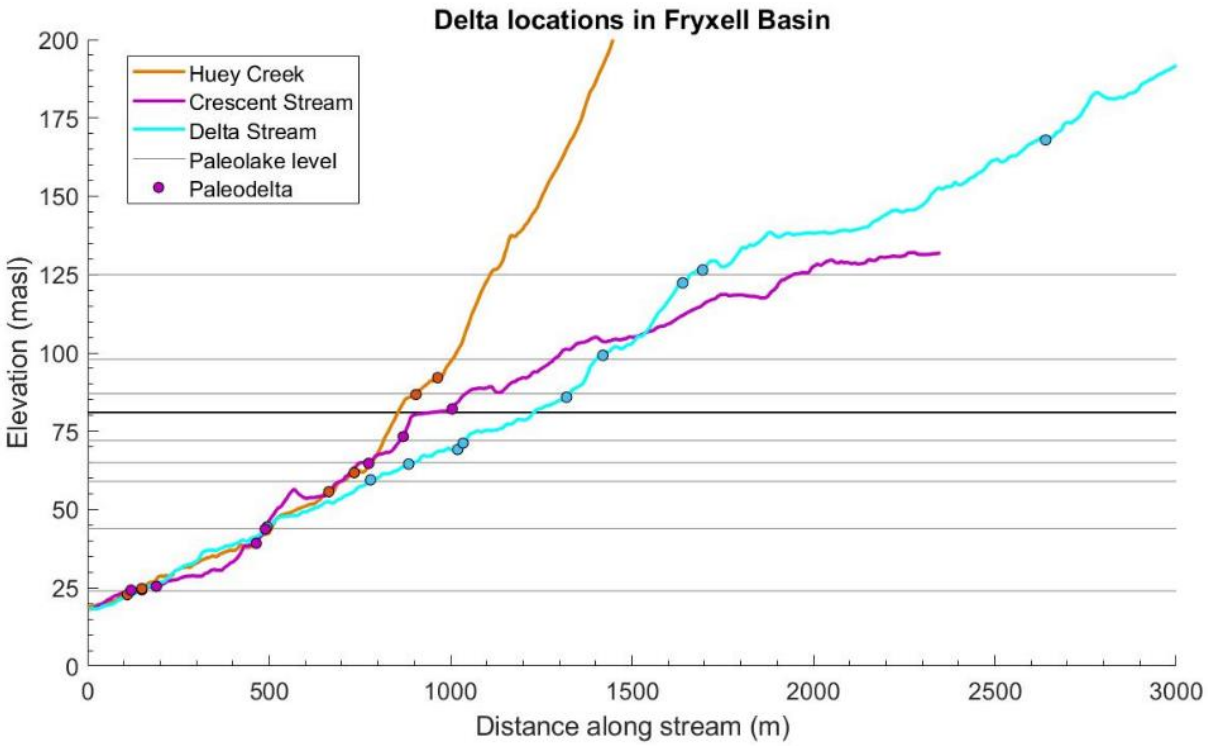

Figure 16. Elevation transects along banks of Huey Creek (orange), Crescent Stream (magenta), and Delta Stream (blue). Locations of mapped paleodeltas on each stream shown as circles. Lake level elevations shown as grey reference lines, and 81 masl reference line is bolded.

Airborne resistivity data was used to map groundwater and permafrost extent within Fryxell basin. A large low resistivity region extends hundreds of meters away from the modern lake extent and is interpreted as a degrading groundwater thaw bulb of GLW since the LGM (**Figure 17**).

In addition to mapping groundwater, higher resistivities overlaying low resistivity brine in the valley floor are interpreted as regions of permafrost which range from ~5 m thick around the lake edge to over 200 m thick higher up on the valley walls (**Figure 18**). Following lake level drop, newly exposed substrate would begin to freeze from the top down.

Permafrost thickness was determined by calculating depth to brine values for Fryxell basin. We use a 100 Ωm threshold to delineate between groundwater and permafrost. Permafrost thickness is lowest near the modern lake edge and increases with increasing distance from lake edge (**Figure 19**). Permafrost thickness has two peaks, one that is <20 m thick (near lake edge) and another peak around 150 to 200 m which occurs further up the valley walls (**Figure 20**). Permafrost resistivity varies depending on water content and temperature. Confining permafrost generally has values >10,000 Ωm, which is seen in only some regions of Fryxell basin. A lower resistivity permafrost layer (between 100 to 1,000 Ωm) extends from the brine layer to approximately 81 masl (**Figure 18**).

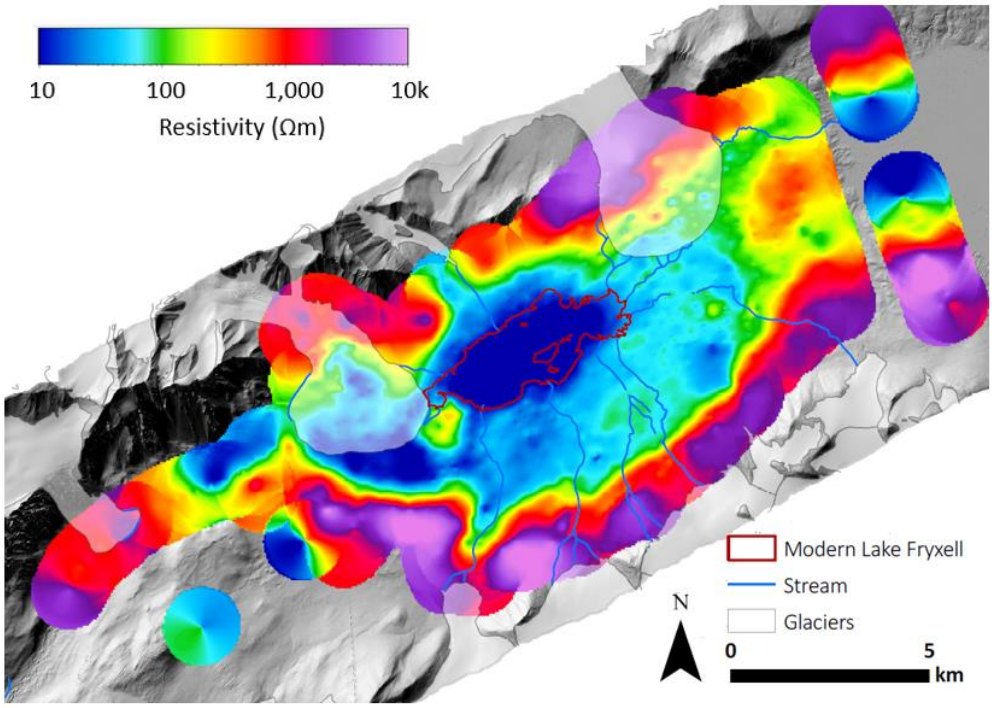

Figure 17. Mean resistivity map of constant elevation (-100 masl, 5 m thick slice) generated from SkyTEM data. DEM (1 m resolution) is from 2014-15 LiDAR survey, accessed via OpenTopography (Fountain et al., 2017).

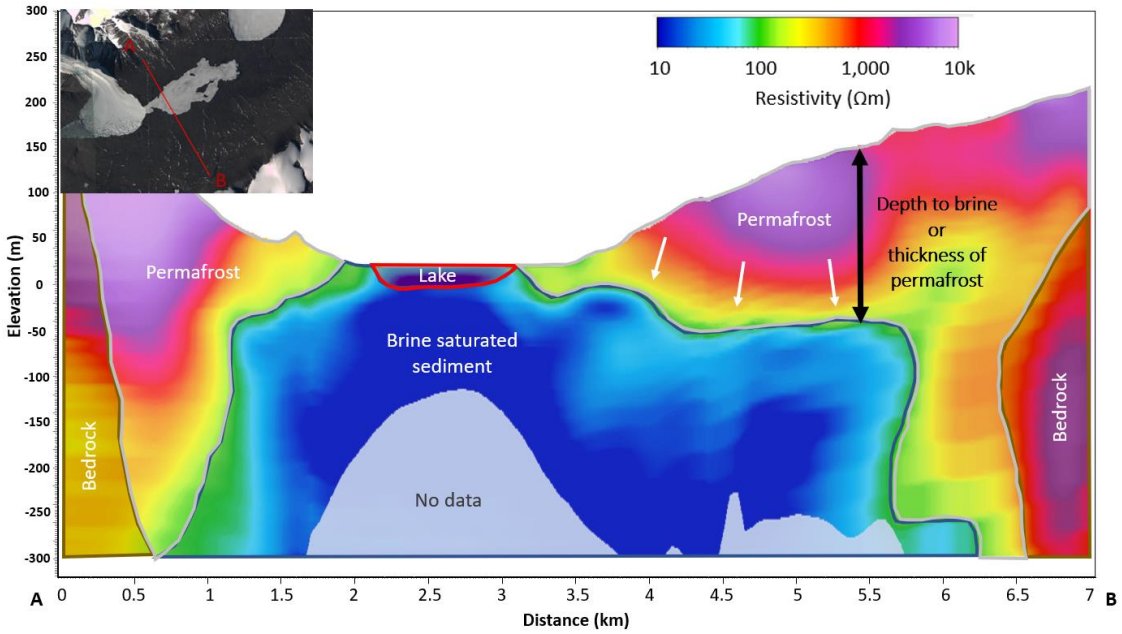

Figure 18. North-south transect created from 3D grid. Mean resistivity maps created using 1 km search radius (2x line spacing), 5 m elevation slices. Interpretations of subsurface conditions based on Mikucki et al. (2015).

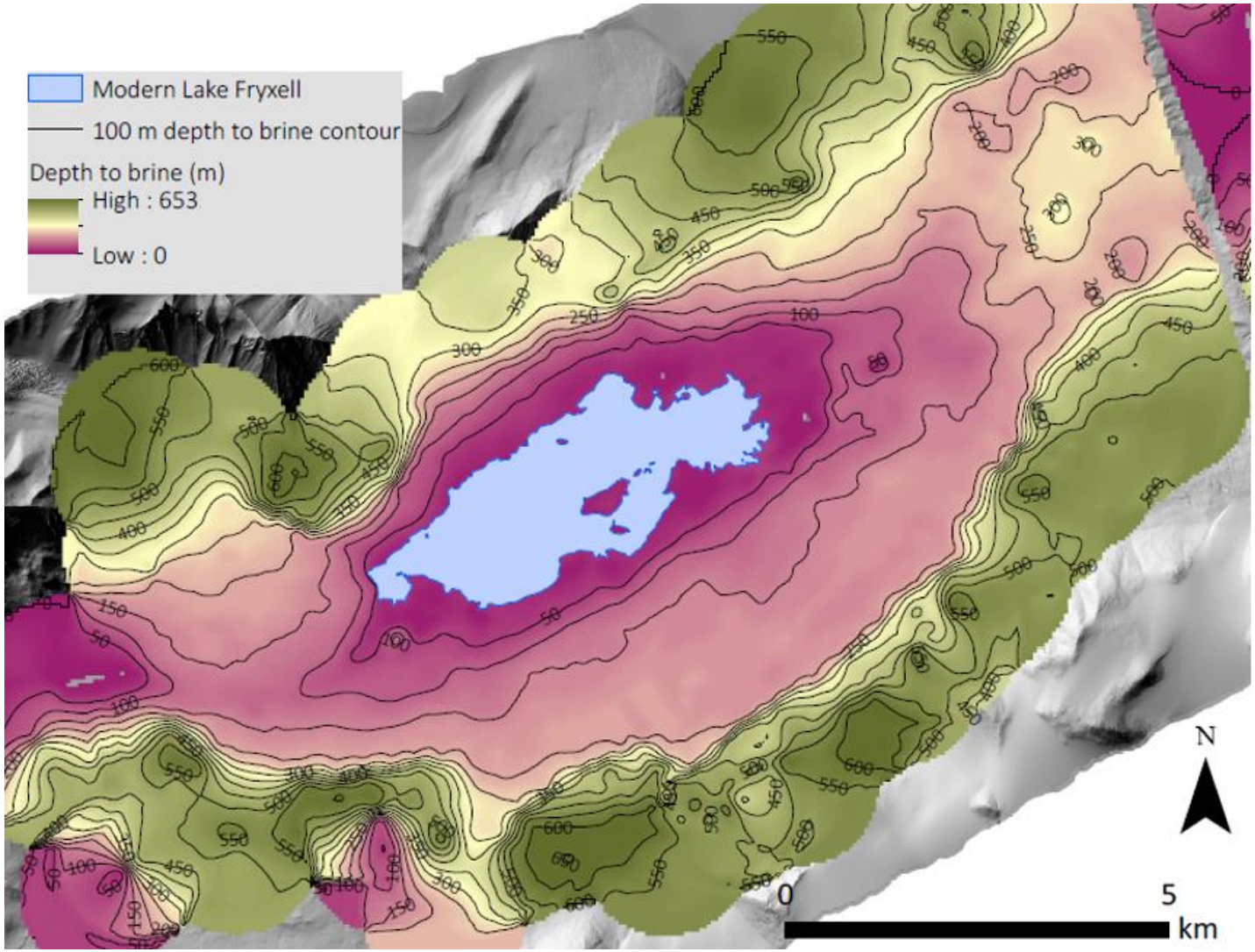

Figure 19. Map showing depth to 100 Ωm brine/permafrost boundary. Interpolation was smoothed using a low pass filter in ArcGIS to reduce edge noise. Edges (higher elevations and deeper brine layers) are less reliable because of inversion interpolation and limitations of depth of investigation.

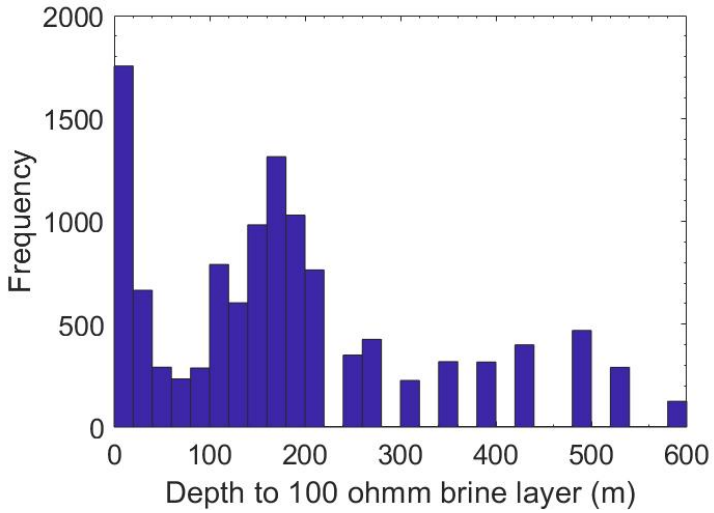

Figure 20. Frequency plot of depth to 100 Ωm brine/permafrost boundary in Fryxell basin.

The presence of a large paleolake during the Holocene would have altered the thermal regime of inundated regions, allowing for a broader groundwater connection. In polar regions, ubiquitous permafrost isolates surface water fluxes from deeper groundwater systems by forming a relatively impermeable layer. Modern conditions in Lake Fryxell maintain an open talik (**Figure 21)**, which is supported by low resistivities indicating lack of permafrost below Lake Fryxell. When lake levels were much higher, a talik would have existed beneath GLW, forming a widespread groundwater connection throughout much of TV. As the lake level dropped to modern levels, sediment became exposed to low atmospheric temperatures and began to freeze. The relic limnological signal is not in a steady state and is interpreted to be in a transient period of gradual freeze-back which will continue until equilibrium is reached.

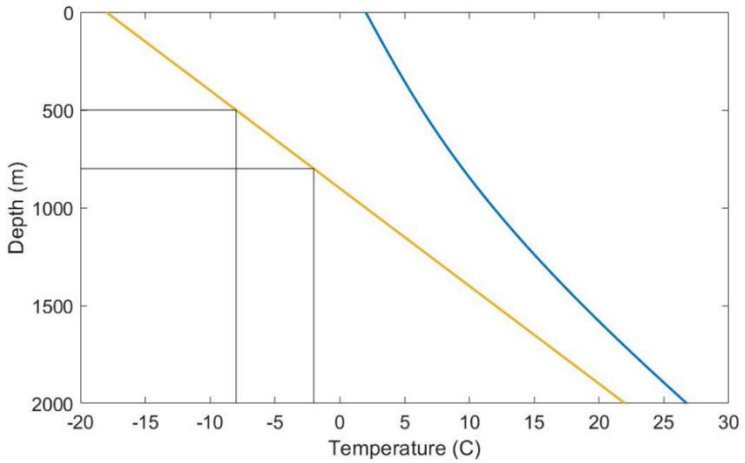

Figure 21. Thermal profile of subsurface beneath Lake Fryxell (blue) using Equation 4 compared to estimated thermal profile of bare ground in TV (yellow) using Equation 5. Black references lines show range of depths (500 – 800 m) that would allow for liquid water to exists from the geothermal gradient alone (assuming a brine freezing point between -2 to -8 C).

First order calculations indicated 1 to 0.5 ka BP permafrost ages, suggesting lake level high-stands in the late Holocene. Monte Carlo statistical analysis was performed to calculate possible ranges for permafrost ages versus elevations by assigning a variance for each input variable (**Figure 22**).

Lower depth to brine values (thinner permafrost) yields a smaller range in possible ages, and uncertainty increases with increasing depth to brine (**Figure 23**). Maximum permafrost ages for partially saturated conditions (24% air in porespace) yielded slightly older ages compared

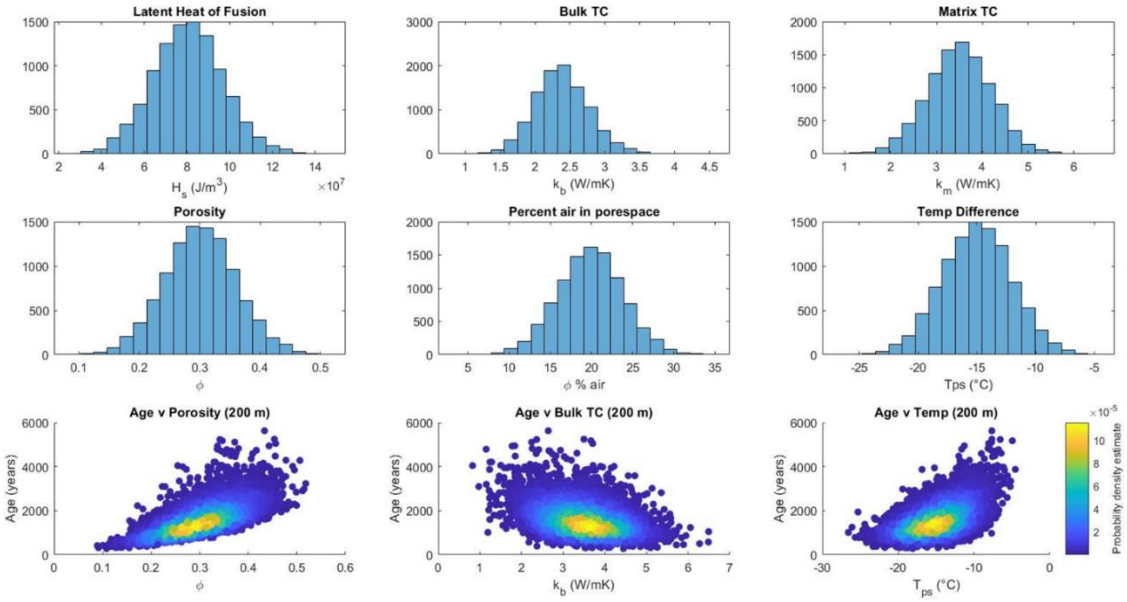

Figure 22. Monte Carlo sensitivity analysis of permafrost age inputs, 10,000 iterations. Bottom scatter plots show how age varies with porosity, bulk TC, and temperature.

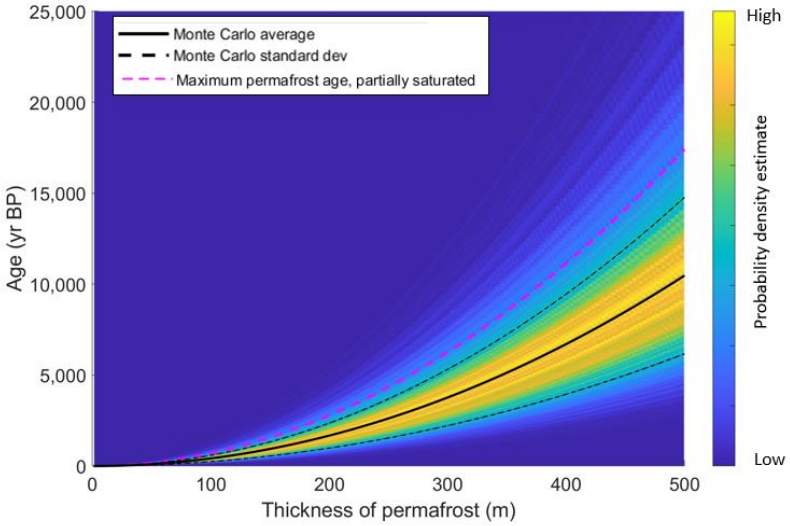

Figure 23. Monte Carlo age versus elevation; average result shown as solid black line, 1 standard deviation as dashed black line. Permafrost ages for maximum inputs (dashed pink) into Eq 1, for saturated conditions (24% air in pore space).

to the first order calculation using average inputs and fully saturated conditions, resulting in a ~500 year increase in age (roughly 1.5 to 1 ka BP) (**Figure 24**).

Depth to brine for each sounding point was used to calculate permafrost age and plotted as a function of sounding point elevation to compare to ^{14}C and OSL ages at corresponding elevations. A comparison of all three methods shows that even maximum permafrost age calculations cannot reproduce ^{14}C ages of paleodeltas from Hall and Denton (2000). OSL dates are still older than permafrost calculations, however there is overlap between the OSL and permafrost ages for higher elevations (**Figure 25**).

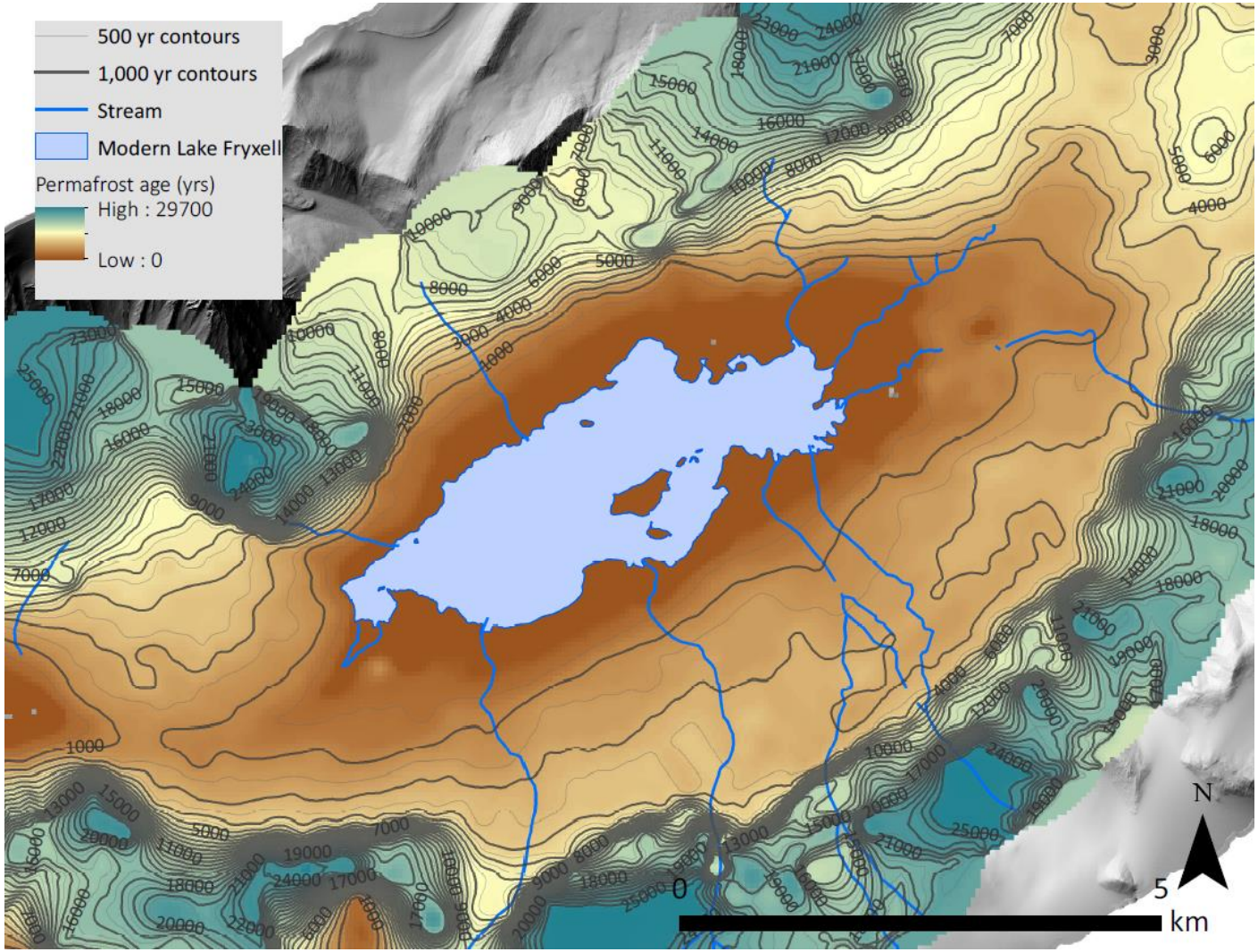

Figure 24. Maximum permafrost age distribution in Fryxell basin using depth to permafrost-brine boundary (defined as 100 Ωm) . Contours represent age of permafrost in years before present, implying recent drainage of GLW during the late Holocene.

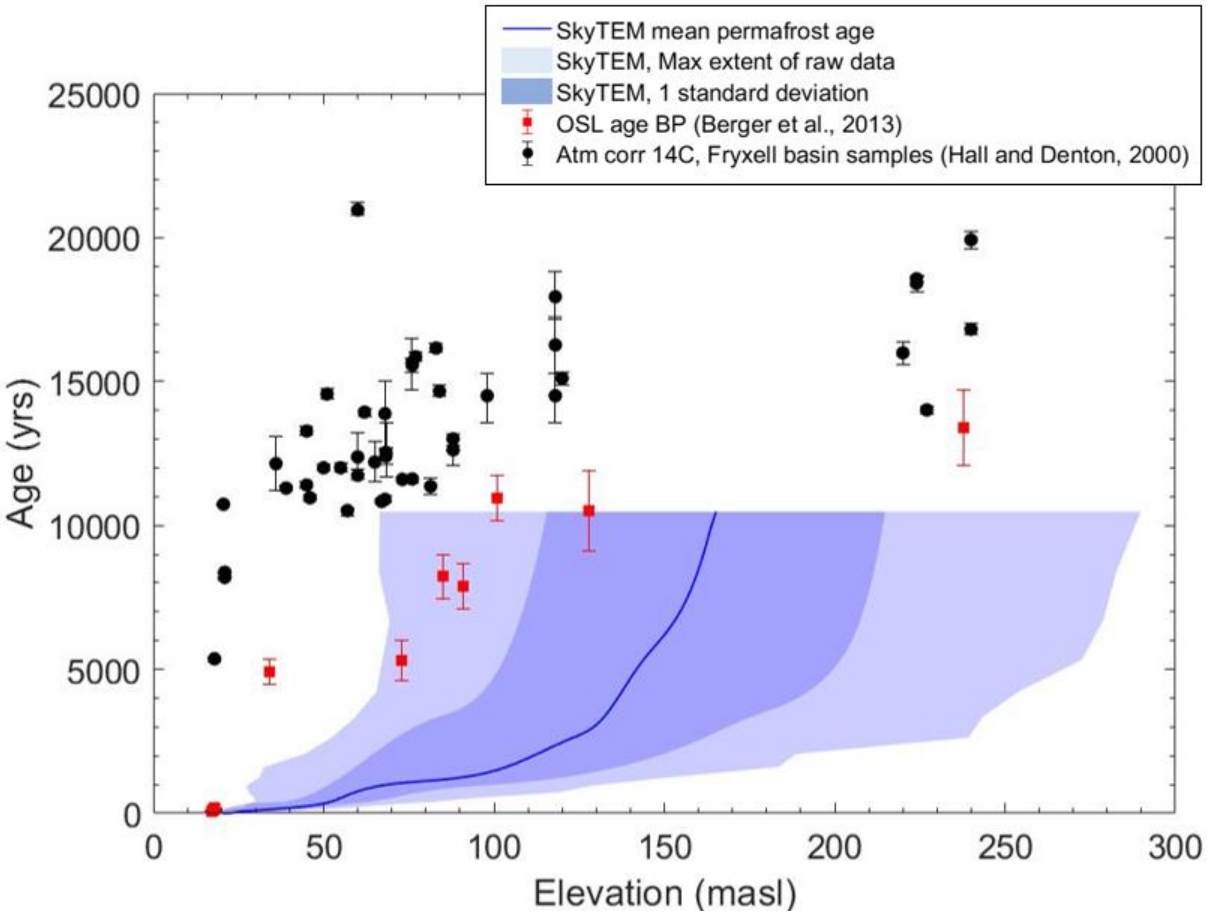

Figure 25. Permafrost ages calculated using SkyTEM resistivity data compared to ^{14}C and OSL ages (Hall and Denton, 2000, Berger et al., 2013). Mean permafrost age for each elevation is plotted as solid blue line, one standard deviation from mean plotted as blue shading, and maximum extent of raw data plotted as light blue shading.

DISCUSSION

Lake levels in TV have fluctuated in the past, leaving behind a complex history of lacustrine deposits and thermal signatures. A novel approach using improved mapping of paleodeltas and SkyTEM resistivity surveys provides new evidence in support of the existence of GLW by constraining lake level timing and extent.

A low resistivity groundwater signal extends hundreds of meters away from modern lake edge and is interpreted as the degrading thaw bulb from GLW. Calculations of the thermal profile below Lake Fryxell paired with SkyTEM resistivity data indicate a talik exists directly below the lake. Relic groundwater systems that formed during lake level high-stands are not in steady state and are actively freezing back until a new equilibrium is reached. This groundwater system is overlaid by regions permafrost, which can be used to calculate time since lake drainage using Equation 1. This conceptual model assumes a constant rate of lake level drop and constant T_{ps} for simplification. Lateral heat flux from modern and ancient lakes is not addressed in this study, however may be important to understand equilibrium thresholds for this evolving groundwater system.

Permafrost age calculations indicate late Holocene lake level high-stands roughly 1.5 to 1 ka BP. With inputs turned to maximize permafrost ages, it was still not possible to yield ages for lake occupation comparable to those estimated by ^{14}C ages of delta deposits (Hall and Denton, 2000). OSL dates roughly fall within the range of ages calculated from the resistivity data (**Figure 23**). Permafrost ages span a wide range of elevations because the depth to brine boundary only roughly follows surface topography. This is probably an indication of subsurface heterogeneity which is also apparent in resistivity maps. Shallower depth to brine values (younger ages) are better constrained compared to older and higher elevation brines as suggested by Monte Carlo statistical analysis and can be used as a rough estimate of uncertainty (**Figure 23**).

Maximum permafrost age calculations paired with paleotemperature records from Taylor Dome can be used to correlate paleoclimate events with hydrologic responses. Lake levels were probably highest around 12 ka BP (OSL date from ~250 masl), the end of a warming period from 15 to 12 ka BP. Lake levels likely dropped from 12 to 8 ka BP due to the retreat of the grounded RIS from the mouth of TV, which was completely removed by 8 ka BP. After the removal of the ice dam lake levels would not be able to exceed 81 masl.

Radiocarbon dating from Hall and Denton (2000) suggests that lake level highstands occurred between 22 to 5 ka BP, and that levels did not exceed modern lake elevation after 5 ka BP. OSL dates (Berger et al., 2013) estimate past lake level high stands existed between 12 – 5 ka BP, and do not suggest very recent lake level increase. We suggest that a radiocarbon reservoir effect may be responsible for the systematic offset of OSL and permafrost ages by 5 to 10 ka. If radiocarbon dates are reduced by a conservative estimate of 5 ka, both OSL and ^{14}C estimates agree with a drainage event associated with the removal of the RIS around 8 ka BP when lake levels dropped to or below the 81 masl sill threshold.

Other studies focusing on the paleolimnology of Lake Fryxell basin suggest Holocene draw down events; however, the magnitude and timing of these events are somewhat contradictory. Lyons et al. (1998) calculates that Lake Fryxell desiccated into a small (7 m deep) pond in the late Holocene. The stable isotope record indicates that bottom waters are depleted in $\delta^{18}O$ and δD with depth suggesting loss of ice cover and partial desiccation prior to 2.6 to 0.65 ka BP followed

by refilling between 1.2 and 1 ka BP. A partial desiccation event cannot be resolved using paleodelta or resistivity data from this study. Paleodeltas would be obscured by modern lake levels, and any permafrost freeze-back signature from drainage would be reset by the modern talik. Sediment cores taken from the bottom of Lake Fryxell do not record a desiccation event, and instead carbonate layers suggest only 4 episodes of significant lake level draw down (6.4, 4.7, 3.8 and 1.6 ka BP) which would have been no more than 3 – 4.5 m below modern lake level (Whittaker et al., 2008). The suggested partial desiccation of Lake Fryxell during the Holocene is therefore considered inconclusive.

Multiple lines of evidence support the maximum permafrost age calculation. Permafrost at approximately 81 masl falls between the 1.5 to 1 ka BP age contours. Taylor Dome ice core records show a highly variable Holocene, with a peak of 6°C above modern temperature around 1.2 ka BP. Timing also corresponds to the elevation and location of a large and very well-preserved delta on Crescent Stream in Fryxell basin. Defined delta structures with nearly zero slope and sharp transitions between the topset and foreset suggest low degrees of weathering. Weathering of delta deposits has not been rigorously addressed in previous literature; however, through visual comparison most deltas are less defined, and the delta on Crescent Stream is the best preserved delta in the basin. Because this delta occurs at 81 masl, the maximum possible lake level without grounded ice at the mouth of TV, it probably formed through multiple cycles of filling and drainages. The combination of a highly preserved delta deposit at 81 masl, the approximate permafrost age of 1.5 to 1 ka BP, and a peak in temperatures (6°C warmer than modern) between 1 to 2 ka BP, suggests that it was possible for lake level be at the sill level at some time in the past 2,000 years (**Figure 26**).

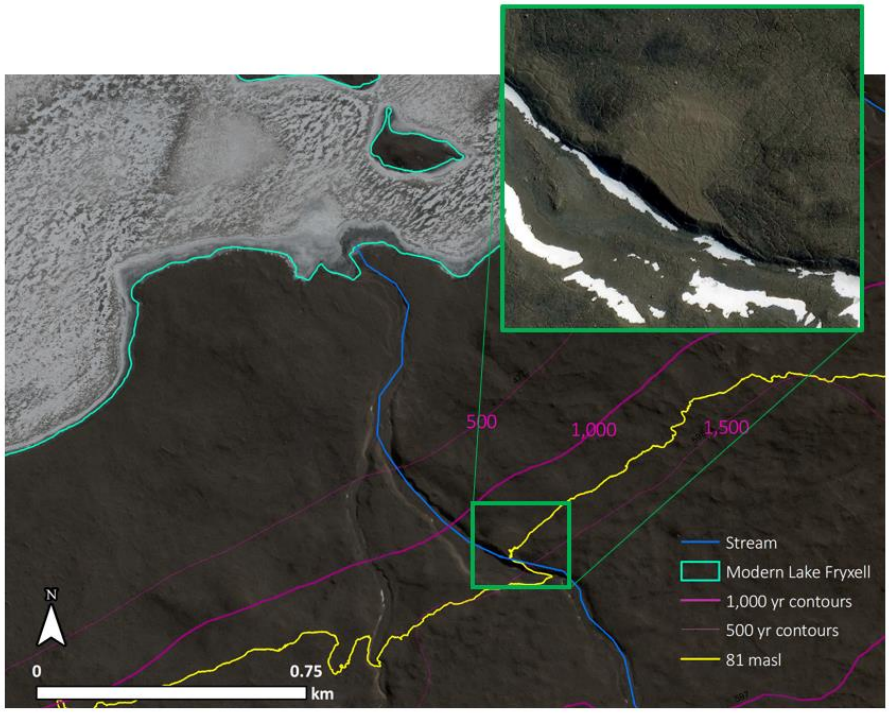

Figure 26. Maximum permafrost age contours (pink) indicate roughly 1.5 to 1 ka BP permafrost at 81 masl (yellow). An extremely well-preserved delta on Crescent Stream is located at roughly 81 masl shown in inset map (green).

CONCLUSIONS

This study provides new insight on lake level evolution in TV. Lake levels were higher during the LGM when an ice dam blocked the mouth of TV, allowing for lake levels to increase by over 280 m compared to modern level. Taylor Dome ice core records indicate an abrupt warming of >15°C from 15 – 12 ka BP, (Steig et al., 2000) (**Figure 2**), which may coincide with maximum lake level of GLW. Following ice sheet retreat approximately 8 ka BP, GLW drained and lake level likely fluctuated between 0 and 81 masl between 8 to 1.5 ka BP. Around 1.5 – 1 ka BP, lake levels were at the 81 masl sill level (**Figure 24**) and have subsequently dropped to at or below modern levels.

Short lived changes in temperature such as the 6°C increase in the late Holocene could have resulted in anywhere between 60 to 80 m of lake level rise and subsequent drainage. Closed basin MDV lakes are characterized by high variability and extreme sensitivity to both climate and geologic drivers. Modern and paleohydrologic evidence indicates a highly dynamic system in which small temperature forcings can initiate a large scale hydrologic response.

REFERENCES

Anderson, J.B., Conway, H., Bart, P.J., Witus, A.E., Greenwood, S.L., McKay, R.M., Hall, B.L., Ackert, R.P., Licht, K., Jakobsson, M., & Stone, J.O. Ross Sea paleo-ice sheet drainage and deglacial history during and since the LGM. Quat. Sci. Rev. 100, 31–54 (2014).

Anderson, J.B., Wilson, G.S., Fink, D., Lilly, K., Levy, R.H., & Townsend, D. Reconciling marine and terrestrial evidence for post LGM ice sheet retreat in southern McMurdo Sound, Antarctica. Quat. Sci. Rev. 157, 1–13 (2016).

Arcone, S.A., Delaney, A.J., Prentice, M.L., & Horsman, J.L. GPR reflection profiles of sedimentary deposits in lower Taylor Valley, Antarctica, paper presented at Twelfth International Conference on Ground Penetrating Radar, Birmingham, United Kingdom, 15–19 June. (2008)

Baroni, C. & Hall, B.L. A new Holocene relative sea-level curve for Terra Nova Bay, Victoria Land, Antarctica. J. Quat. Sci. 19, 377–396 (2004).

Berger, G. W., Doran, P.T., & Thomsen, K.J. Micro-hole and multigrain quartz luminescence dating of Paleodeltas at Lake Fryxell, McMurdo Dry Valleys (Antarctica), and relevance for lake history. Quat. Geochronol. 18, 119–134 (2013).

Bockheim, J., Campbell, I. & McLeod, M. Permafrost Distribution and Active-Layer Depths in the McMurdo Dry Valleys, Antarctica. Permafr. Periglac. Process. (2007)

Cartwright, K. & Harris H.J.H. Hydrogeology of the Dry Valley Region, Antarctica. In: McGinnis L (ed) Dry Valley Drilling project. Antarctic Research Series, AGU, Washington, DC, pp 193–214 (1981).

Clayton-Greene, J.M., Hendy, C.H., & Hogg, A.G. Chronology of a Wisconsin age proglacial lake in the Miers Valley, Antarctica. New Zeal. J. Geol. Geophys. 31, 353–361 (1988).

Chinn, T.J.H. Accelerated Ablation at a Glacier Ice-Cliff Margin, Dry Valleys, Antarctica. INSTAAR, Univ. Color. 19, 71–80 (1987).

Cunningham, W.L., Leventer, A., Andrews, J.T., Jennings, A.E., & Licht, K.J. Late Pleistocene-Holocene marine conditions in the Ross Sea, Antarctica: Evidence from the diatom record. Holocene 9, 129–139 (1999).

Denton, G.H. & Marchant, D.R. The Geologic Basis for a Reconstruction of a Grounded Ice Sheet in McMurdo Sound, Antarctica, at the Last Glacial Maximum. Geogr. Ann. Ser. A, Phys. Geogr. 82, 167–211 (2000).

Dickinson, W.W. & Rosen, M.R. Antarctic permafrost: An analogue for water and diagenetic minerals on Mars. Geology 31, 199–202 (2003).

Dickson, J. L., Head, J. W., Levy, J. S. & Marchant, D. R. Don Juan Pond, Antarctica: Near-surface CaCl(2)-brine feeding Earth's most saline lake and implications for Mars. Sci. Rep. 3, 1166 (2013).

Doran, P.T., Wharton, R.A., Des Marais, D.J. & McKay, C.P. Antarctic paleolake sediments and the search for extinct life on Mars. J. Geophys. Res. 103, 28481 (1998).

Doran, P.T., Berger, G.W., Lyons, W.B., Wharton, R.A., Divisson, M.L., Southon, & J., Dibb, J.E. Dating Quaternary lacustrine sediments in the McMurdo Dry Valleys, Antarctica. Palaeogeogr. Palaeoclimatol. Palaeoecol. 147, 223–239 (1999).

Doran, P.T., McKay, C.P., Clow, G.D., Dana, G.L., Fountain, A.G., Nylen, T., & Lyons, W.B. Valley floor climate observations from the McMurdo dry valleys, Antarctica, 1986-2000. J. Geophys. Res. Atmos. 107, 1–12 (2002).

Doran, P.T., McKay, C.P., Fountain, A.G., Nylen, T., McKnight, D.M., Jaros, C., & Barret, J.E. Hydrologic response to extreme warm and cold summers in the McMurdo Dry Valleys, East Antarctica. Antarct. Sci. 20, 499–509 (2008).

Doran, P.T., Kenig, F., Lawson Knoepfle, J., Mikucki, J. & Lyons, W.B. Radiocarbon distribution and the effect of legacy in lakes of the McMurdo Dry Valleys, Antarctica. Limnol. Oceanogr. 59, 811–826 (2014).

Dort, W. Climatic causes of alpine glacier fluctuation, southern Victoria Land. Int. Assoc. Sci. Hydrol. SCAR Publ. 86, 358–362 (1970).

Dugan, H., Obryk, M. & Doran, P.T. Lake ice ablation rates from permanently ice-covered Antarctic lakes. J. Glaciol. 59, (2013).

Ebnet, A., Fountain, A. G., Nylen, T. H., McKnight, D. M. & Jaros, C. L. A temperature-index model of stream flow at below-freezing temperatures in Taylor Valley, Antarctica. Ann. Glaciol. 40, 76–82 (2005).

Foley, N. et al. Helicopter-borne transient electromagnetics in high-latitude environments: An application in the McMurdo Dry Valleys, Antarctica. Geophysics 81, WA87-WA99 (2016).

Fountain, A.G., Nylen, T.H., Monaghan, A., Basagic, H.J. & Bromwich, D. Snow in the McMurdo Dry Valleys, Antarctica. Int. J. Climatol. 30, 633–642 (2010).

Fountain, A.G. et al. The Impact of a Large-Scale Climate Event on Antarctic Ecosystem Processes. Bioscience 66, 848–863 (2016).

Fountain, A.G., Fernandez-Diaz, J.C., Obryk, M., Levy, J., Gooseff, M., Van Horn, D.J., Morin, P., & Shrestha, R. High-resolution elevation mapping of the McMurdo Dry Valleys, Antarctica, and surrounding regions, Earth Syst. Sci. Data, 9, 435-443 (2017).

Hall, B.L. & Denton, G.H. Radiocarbon chronology of Ross Sea drift, eastern Taylor Valley, Antarctica; evidence for a grounded ice sheet in the Ross Sea at the last glacial maximum. Geogr. Ann. Ser. A Phys. Geogr. 82, 305–336 (2000).

Hall, B.L., Denton, G.H. & Overturf, B. Glacial Lake Wright, a high-level Antarctic lake during the LGM and early Holocene. Antarct. Sci. 13, 53–60 (2001).

Hall, B. L. & Henderson, G.M. Use of uranium-thorium dating to determine past 14C reservoir effects in lakes: Examples from Antarctica. Earth Planet. Sci. Lett. 193, 565–577 (2001).

Hall, B.L., Denton, G.H., Overturf, B. & Hendy, C.H. Glacial Lake Victoria, a high-level Antarctic lake inferred from lacustrine deposits in Victoria Valley. J. Quat. Sci. 17, 697–706 (2002).

Hall, B.L., Baroni, C. & Denton, G.H. Holocene relative sea-level history of the Southern Victoria Land Coast, Antarctica. Glob. Planet. Change 42, 241–263 (2004).

Hall, B.L. Holocene glacial history of Antarctica and the sub-Antarctic islands. Quat. Sci. Rev. 28, 2213–2230 (2009).

Hall, B.L., Denton, G.H., Heath, S.L., Jackson, M.S. & Koffman, T.N.B. Accumulation and marine forcing of ice dynamics in the western Ross Sea during the last deglaciation: Supplementary Info. Nat. Geosci. 8, 625–628 (2015).

Hendy, C., Sadler, A., Denton, G. & Hall, B. Proglacial Lake-Ice Conveyors : A New Mechanism for Deposition of Drift in Polar Environments. 82, 249–270 (2000).

Hendy, C.H. & Hall, B.L. The radiocarbon reservoir effect in proglacial lakes: Examples from Antarctica. Earth Planet. Sci. Lett. 241, 413–421 (2006).

Horsman, J.L. The origin of sandy terraces in eastern Taylor Valley, Antarctica, from Ground Penetrating Radar: A test of the Glacial Lake Washburn delta interpretation, MS thesis, 258 pp., Plymouth State University, Plymouth, New Hampshire. (2007).

Higgins, S.M., Hendy, C.H. & Denton, G.H. Geochronology of Bonney Drift, Taylor Valley, Antarctica: Evidence for interglacial expansions of Taylor Glacier. Geogr. Ann. Ser. A Phys. Geogr. 82, 391–409 (2000).

Konfal, S.A., Wilson, T.J. & Hall, B.L. Palaeoshoreline records of glacial isostatic adjustment in the Dry Valleys region, Antarctica. Geol. Soc. London, Spec. Publ. 381, 455–467 (2013).

Levy, J.S., Head, J.W., Marchant, D.R., Dickson, J.L. & Morgan, G.A. Geologically recent gully-polygon relationships on Mars: Insights from the Antarctic Dry Valleys on the roles of permafrost, microclimates, and water sources for surface flow. Icarus 201, 113–126 (2009).

Levy, J.S., Fountain, A.G., Gooseff, M.N., Welch, K.A. & Lyons, W.B. Water tracks and permafrost in Taylor Valley, Antarctica: Extensive and shallow groundwater connectivity in a cold desert ecosystem. Bull. Geol. Soc. Am. 123, 2295–2311 (2011).

Levy, J. How big are the McMurdo Dry Valleys? Estimating ice-free area using Landsat image data. Antarct. Sci. 25, 119–120 (2013).

Lyons, W.B., Tyler, S.W., Wharton, R.A., McKnight, D.M. & Vaughn, B.H. A Late Holocene desiccation of Lake Hoare and Lake Fryxell, McMurdo Dry Valleys, Antarctica. Antarct. Sci. 10, 247–256 (1998).

Lyons, W.B., Fountain, A., Doran, P.T., Priscu, J.C., Neumann, K., & Welch, K.A., Importance of landscape position and legacy: The evolution of the lakes in Taylor Valley, Antarctica. Freshw. Biol. 43, 355–367 (2000).

McGinnis, L.D. & Jensen, T.E. Permafrost-Hydrogeologic Regimen in Two Ice-Free Valleys, Antarctica, from Electrical Depth Soundings. 389–409 (1971).

Mikucki, J.A., Auken, E., Tulaczyk, S., Virginia, R.A., Schamper, C., Sorensen, K.I., Doran, P.T., Dugan, H., & Foley, N. Deep groundwater and potential subsurface habitats beneath an Antarctic dry valley. Nat. Commun. 6, 6831 (2015).

Obryk, M.K., Doran, P.T., Waddington, E.D. & McKay, C.P. The influence of föhn winds on Glacial Lake Washburn and palaeotemperatures in the McMurdo Dry Valleys, Antarctica, during the Last Glacial Maximum. Antarct. Sci. 29, 457–467 (2017).

Osterkamp, T.E. & Burn, C.R. Permafrost, in Encyclopedia of Atmospheric Sciences, edited by J. R. Holton, pp. 1717–1729, Academic, Oxford, U.K. (2003).

Reimer, P., Baillie, M. & Bard, E. IntCal04 terrestrial radiocarbon age calibration, 0-26 cal kyr BP. Radiocarbon 46, 1029–1058 (2004).

Scott, R.F., The Voyage of the 'Discovery', C. Scribner's Sons, New York (1905).

Spector, P., Stone, J., Cowdery, S.G., Hall, B., Conway, H., & Bromley, G. Rapid early-Holocene deglaciation in the Ross Sea, Antarctica. Geophys. Res. Lett. 44, 7817–7825 (2017).

Steig, E.J., Morse, D.L., Waddington, E.D., Stuiver, M., Grootes, P.M., Mayewski, P.A., Twickler, M.S., & Whitlow, S.I. Wisconsinan and Holocene Climate History from an Ice Core at Taylor Dome, Western Ross Embayment, Antarctica. Geogr. Ann. Ser. A Phys. Geogr. 82A, 213–235 (2000).

Stuiver, M., Denton, G.H., Hughes, T.J., & Fastook, J.L. History of the marine ice sheet in West Antarctica during the last glaciation: A working hypothesis. *In*: Denton, G.H. and Hughes, T.J. (eds): The Last Great Ice Sheets. John Wiley and Sons. New York. 319-436 (1981).

Stuiver, M., Reimer, P.J., & Reimer, R.W. CALIB 7.1 [WWW program] at http://calib.org, accessed 2018-6-4 (2018).

Sudman, Z., Gooseff, M.N., Fountain, G.A., Levy, J.S., Obryk, M.K., & Van Horn, D. Impacts of permafrost degradation on a stream in Taylor Valley, Antarctica. Geomorphology 285, 205–213 (2017).

Toner, J.D., Sletten, R.S. & Prentice, M.L. Soluble salt accumulations in Taylor Valley, Antarctica: Implications for paleolakes and Ross Sea Ice Sheet dynamics. J. Geophys. Res. Earth Surf. 118, 198–215 (2013).

Ward, S.H. & Hohmann G.W. Electromagnetic theory for geophysical applications, in M. N. Nabighian, ed., Electromagnetic methods in applied geophysics: SEG, 130–311. (1988).

VITA

Krista Falcon Myers grew up in coastal California and received her bachelor's degree from the University of California, Santa Cruz. As an undergraduate, Krista became involved in glaciology research which is ultimately what inspired her to pursue a graduate degree studying the cryosphere. During her graduate tenure, Krista conducted three seasons of field work in the McMurdo Dry Valleys, totaling 154 days of sleeping on the ground in Antarctica. After receiving her master's degree from LSU, she plans to continue to study the cryosphere and dedicate her life to increasing awareness and solving problems related to climate change.